UNITED NATIONS EDUCATIONAL, SCIENTIFIC AND CULTURAL ORGANIZATION
INTERNATIONAL ATOMIC ENERGY AGENCY
INTERNATIONAL CENTRE FOR THEORETICAL PHYSICS
I.C.T.P., P.O. BOX 586, 34100 TRIESTE, ITALY, CABLE: CENTRATOM TRIESTE

SMR/1003 - 3

SUMMER COLLEGE IN CONDENSED MATTER ON
" STATISTICAL PHYSICS OF FRUSTRATED SYSTEMS "

(28 July - 15 August 1997)

" Coarsening, aging and persistence"

presented by:

A.J. BRAY
University of Manchester
Dept. of Physics and Astronomy
Manchester M13 9PL
United Kingdom

COARSENING, AGING AND PERSISTENCE

A. J. Bray

Department of Physics and Astronomy
University of Manchester
Manchester M13 9PL, UK

Contents

1 Introduction

An essential feature of the dynamics of frustrated disordered systems (or even some nonfrustrated disordered systems) is that, in the low-temperature phase, macroscopic systems do not reach equilibrium in the timescales available to experimentalists. Understanding such systems, therefore, necessarily involves studying the *nonequilibrium* dynamics of the ordered phase. Indeed, even in pure systems this is true in the thermodynamic limit if the system is cooled through the transition temperature at any finite rate. The latter is the subject of 'phase-ordering kinetics'. In these lectures I shall begin with the nonequilibrium dynamics of pure systems, introducing the concepts of coarsening and aging in this simple context. I will then discuss how the results are modified in nonfrustrated disordered systems, where the disorder provides a pinning barrier to the motion of the domain boundaries between different pure states. For frustrated disordered systems, notably spin glasses, the question of the number of such pure states has not been definitively settled for finite-dimensional systems. I will introduce the simple 'droplet model', with only two pure phases, and use it to discuss the nonequilibrium dynamics of spin glasses in a manner motivated by the earlier study of pure and nonfrustrated disordered systems. Finally, the phenomenon of 'persistence' will be introduced and briefly discussed in the context of pure systems. A more complete discussion of the material in section II can be found be found in a recent review [1], while much of the material on the droplet model is based on an earlier review [2].

2 Coarsening of Pure Systems

Systems cooled from a disordered phase into an ordered phase do not order instantaneously. Instead, the length scale of ordered regions grows with time as the different broken symmetry phases compete to select the equilibrium state. To fix our ideas, it is helpful to consider the simplest, and most familiar, system: the ferromagnetic Ising model. Consider a temperature quench, at time $t = 0$, from an initial temperature T_I above the critical point T_C to a final temperature T_F below T_C. At T_F there are two equilibrium phases, with magnetization $\pm M_0$. Immediately after the quench, however, the system is in an unstable disordered state corresponding to equilibrium at temperature T_I. The theory of 'phase-ordering kinetics' is concerned with the dynamical evolution of the system from the initial disordered state to the final equilibrium state.

It is important to realize that, in the thermodynamic limit, final equilibrium is never achieved! This is because the longest relaxation time diverges with the system size in the ordered phase, reflecting the broken ergodicity. Instead, a pattern of domains of the equilibrium phases develops, and the typical length scale associated with these domains increases with time t. This situation is illustrated in Figure 1, which shows a Monte Carlo simulation of a two-dimensional Ising model, quenched from $T_I = \infty$ to $T_F = 0$. Inspection of the time sequence may persuade you that domain coarsening is a *scaling* phenomenon – the domain patterns at later times look statistically similar to those at earlier times, apart from a global change of scale. This 'dynamic scaling hypothesis' will be formalized below.

For pedagogical reasons, we have introduced domain-growth in the context of the Ising model, and will continue to use magnetic language for simplicity. A related phenomenon that has been studied for many decades, however, by metallurgists, is the spinodal decomposition of binary alloys, where the late stages of growth are known as 'Ostwald ripening'. Similar phenomena occur in the phase separation of fluids or binary liquids, although in these cases the phase separation is accelerated by the earth's gravitational field, which severely limits the temporal duration of the scaling regime. The gravitational effect can be moderated by using density-matched binary liquids and/or performing the experiments under microgravity. All of the above systems, however, contain an extra complication not present in the Ising ferromagnet. This is most simply seen by mapping an AB alloy onto an Ising model. If we represent an A atom by an up spin, and a B atom by a down spin,

then the *equilibrium* properties of the alloy can be modelled very nicely by the Ising model. There is one important feature of the alloy, however, that is not captured by the Ising model with conventional Monte-Carlo dynamics. Flipping a single spin in the Ising model corresponds to converting an A atom to a B atom (or vice versa), which is inadmissible. The dynamics must conserve the number of A and B atoms separately, i.e. the magnetization (or 'order parameter') of the Ising model should be *conserved*. This will influence the form of the coarse-grained equation of motion, as discussed in section 2.1 and lead to slower growth than for a non-conserved order parameter.

In all the systems mentioned so far, the order parameter (e.g. the magnetization of the Ising model) is a scalar. In the last few years, however, there has been increasing interest in systems with more complex order parameters. Consider, for conceptual simplicity, a planar ferromagnet, in which the order parameter is a vector confined to a plane. After a quench into the ordered phase, the magnetization will point in different directions in different regions of space, and singular lines (vortex lines) will form at which the direction is not well defined. These 'topological defects' are the analog of domain walls for the scalar systems. An understanding of the relevant topological defects in the system, combined with the scaling hypothesis, provides the basis for understanding the forms of the growth laws and scaling functions for phase ordering in a wide variety of systems.

2.1 Dynamical Models

It is convenient to set up a continuum description in terms of a coarse-grained order-parameter field (e.g. the 'magnetization density') $\phi(\mathbf{x}, t)$, which we will initially take to be a scalar field. A suitable Landau free-energy functional to describe the ordered phase is

$$F[\phi] = \int d^d x \, \left(\frac{1}{2} (\nabla \phi)^2 + V(\phi) \right) \, , \tag{1}$$

where the 'potential' $V(\phi)$ has a double-well structure, e.g. $V(\phi) = (1 - \phi^2)^2$. We will take the minima of $V(\phi)$ to occur at $\phi = \pm 1$, and adopt the convention that $V(\pm 1) = 0$. The two minima of V correspond to the two equilibrium states, while the gradient-squared term in (1) associates an energy cost to an interface between the phases.

In the case where the order parameter is not conserved, an appropriate equation for the time evolution of the field ϕ is

$$\begin{aligned} \partial \phi / \partial t &= -\delta F / \delta \phi \\ &= \nabla^2 \phi - V'(\phi) \, , \end{aligned} \tag{2}$$

where $V'(\phi) \equiv dV/d\phi$. A kinetic coefficient Γ, which conventionally multiplies the right-hand side of (2), has been absorbed into the timescale. Eq. (2), a simple 'reaction-diffusion' equation, corresponds to simple gradient descent, i.e. the rate of change of ϕ is proportional to the gradient of the free-energy functional in function space. This equation provides a suitable coarse-grained description of the Ising model, as well as alloys that undergo an order-disorder transition on cooling through T_C, rather than phase separating. Such alloys form a two-sublattice structure, with each sublattice occupied predominantly by atoms of one type. In Ising model language, this corresponds to antiferromagnetic ordering. The magnetization is no longer the order parameter, but a 'fast mode', whose conservation does not significantly impede the dynamics of the important 'slow modes'.

When the order parameter is conserved, as in phase separation, a different dynamics is required. In the alloy system, for example, it is clear physically that A and B atoms can only exchange locally (not over large distances), leading to diffusive transport of the order parameter, and an equation of motion of the form

$$\begin{aligned} \partial \phi / \partial t &= \nabla^2 \delta F / \delta \phi \\ &= -\nabla^2 \left[\nabla^2 \phi - V'(\phi) \right] \, , \end{aligned} \tag{3}$$

which can be written in the form of a continuity equation, $\partial_t \phi = -\nabla \cdot j$, with current $j = -\lambda \nabla(\delta F/\delta\phi)$. In (3), we have absorbed the transport coefficient λ into the timescale.

Eqs. (2) and (3) are sometimes called the Time-Dependent-Ginzburg-Landau (TDGL) equation and the Cahn-Hilliard equation respectively. A more detailed discussion of them in the present context can be found in the lectures by Langer [3]. The same equations with additional Langevin noise terms on the right-hand sides are familiar from the theory of critical dynamics, where they are 'model A' and 'model B' respectively in the classification of Hohenberg and Halperin [4].

The absence of thermal noise terms in (2) and (3) indicates that we are effectively working at $T = 0$. A schematic Renormalization Group (RG) flow diagram for T is given in Figure 2, showing the three RG fixed points at 0, T_C and ∞, and the RG flows. Under coarse-graining, temperatures above T_C flow to infinity, while those below T_C flow to zero. We therefore expect the final temperature T_F to be an irrelevant variable (in the scaling regime) for quenches into the ordered phase. This can be shown explicitly for systems with a conserved order parameter [5, 6]. For this case the thermal fluctuations at T_F simply renormalize the bulk order parameter and the surface tension of the domain walls: when the characteristic scale of the domain pattern is large compared to the domain wall thickness (i.e. the bulk correlation length in equilibrium), the system behaves *as if* it were $T = 0$, with the temperature dependence entering through T-dependent model parameters.

In a similar way, any short-range correlations present at T_I should be irrelevant in the scaling regime, i.e. all initial temperatures are equivalent to $T_I = \infty$. Therefore we will take the *initial conditions* to represent a completely disordered state. For example, one could choose the 'white noise' form

$$\langle \phi(\mathbf{x}, 0)\, \phi(\mathbf{x}', 0) \rangle = \Delta\, \delta(\mathbf{x} - \mathbf{x}') \;, \tag{4}$$

where $\langle \cdots \rangle$ represents an average over an ensemble of initial conditions, and Δ controls the size of the initial fluctuations in ϕ. The above discussion, however, indicates that the precise form of the initial conditions should not be important, as long as only short-range spatial correlations are present.

The challenge of understanding phase ordering dynamics, therefore, can be posed as finding the nature of the late-time solutions of deterministic differential equations like (2) and (3), subject to random initial conditions. A physical approach to this formal mathematical problem is based on studying the structure and dynamics of the topological defects in the field ϕ.

2.1.1 The Scaling Hypothesis

Although originally motivated by experimental and simulation results for the structure factor and pair correlation function [7, 8, 9, 10] for ease of presentation it is convenient to introduce the scaling hypothesis first, and then discuss its implications for growth laws and scaling functions. Briefly, the scaling hypothesis states that there exists, at late times, a single characteristic length scale $L(t)$ such that the domain structure is (in a statistical sense) independent of time when lengths are scaled by $L(t)$. It should be stressed that scaling has not been proved, except in some simple models such as the one-dimensional Glauber model[11] and the n-vector model with $n = \infty$ [12]. However, the evidence in its favour is compelling. Moreover, it turns out that the scaling hypothesis, together with a result ('Porod's Law' – see below) for the tail of the structure factor, is sufficient to determine the form of $L(t)$ for most cases of interest [23, 24, 1].

Two commonly used probes of the domain structure are the equal-time pair correlation function

$$C(\mathbf{r}, t) = \langle \phi(\mathbf{x} + \mathbf{r}, t)\, \phi(\mathbf{x}, t) \rangle \;, \tag{5}$$

and its Fourier transform, the equal-time structure factor,

$$S(\mathbf{k}, t) = \langle \phi_{\mathbf{k}}(t)\, \phi_{-\mathbf{k}}(t) \rangle \;. \tag{6}$$

Here angle brackets indicate an average over initial conditions. The structure factor can, of course, be measured in scattering experiments. The existence of a single characteristic length scale, according to the scaling hypothesis, implies that the pair correlation function and the structure factor have the scaling forms

$$\begin{aligned} C(\mathbf{r},t) &= f(r/L)\ , \\ S(\mathbf{k},t) &= L^d\, g(kL)\ , \end{aligned} \tag{7}$$

where d is the spatial dimensionality, and $g(y)$ is the Fourier transform of $f(x)$. Note that $f(0) = 1$, since (at $T = 0$) there is perfect order within a domain.

At general temperatures $T < T_c$, $f(0) = M^2$, where M is the equilibrium value of the order parameter. (Note that the *scaling limit* is defined by $r \gg \xi$, $L \gg \xi$, with r/L arbitrary, where ξ is the equilibrium correlation length). Alternatively, we can extract the factor M^2 explicitly by writing $C(\mathbf{r},t) = M^2\, f(r/L)$. The statement that T is irrelevant then amounts to asserting that any remaining temperature dependence can be absorbed into the domain scale L, such that the function $f(x)$ is independent of T. The scaling forms (7) are well supported by simulation data and experiment.

For future reference, we note that the different-time correlation function, defined by $C(\mathbf{r},t,t') = \langle \phi(\mathbf{x}+\mathbf{r},t)\,\phi(\mathbf{x},t')\rangle$, can also be written in scaling form. A simple generalization of (7) gives [13, 14]

$$C(\mathbf{r},t,t') = f(r/L, r/L')\ , \tag{8}$$

where L, L' stand for $L(t)$ and $L(t')$. Especially interesting is the limit $L \gg L'$, when (8) takes the form

$$C(\mathbf{r},t,t') \to (L'/L)^{\bar{\lambda}}\, h(r/L)\ , \qquad L \gg L'\ , \tag{9}$$

where the exponent $\bar{\lambda}$, first introduced by Fisher and Huse in the context of non-equilibrium relaxation in spin glasses [15], is a non-trivial exponent associated with phase ordering kinetics [16]. It has recently been measured in an experiment on twisted nematic liquid crystal films [17]. The *autocorrelation* function, $A(t) = C(\mathbf{0},t,t')$ is therefore a function only of the ratio L'/L, with $A(t) \sim (L'/L)^{\bar{\lambda}}$ for $L \gg L'$.

In the following sections, we explore the forms of the scaling functions in more detail. For scalar fields, for example, the scaling function $f(x)$ is linear for small x, for both conserved and non-conserved dynamics. We shall see that this is a simple consequence of the existence of 'sharp' (in a sense to be clarified), well-defined domain walls in the system. A corollary is that the structure factor scaling function $g(y)$ exhibits a power-law tail, $g(y) \sim y^{-(d+1)}$ for $y \gg 1$, a result known as 'Porod's law' [18, 19]. It can be shown that this result, and its generalization to more complex fields, together with the scaling hypothesis, are sufficient to determine the growth law for $L(t)$ [23, 24, 1].

2.1.2 Domain Walls

It is instructive to first look at the properties of a flat equilibrium domain wall. From (2) the wall profile is the solution of the equation

$$d^2\phi/dg^2 = V'(\phi)\ , \tag{10}$$

with boundary conditions $\phi(\pm\infty) = \pm 1$, where g is a coordinate normal to the wall. We can fix the 'centre' of the wall (defined by $\phi = 0$) to be at $g = 0$ by the extra condition $\phi(0) = 0$. Integrating (10) once, and imposing the boundary conditions, gives $(d\phi/dg)^2 = 2V(\phi)$. This result can be used in (1) to give the energy per unit area of wall, i.e. the surface tension, as

$$\sigma = \int_{-\infty}^{\infty} dg\,(d\phi/dg)^2 = \int_{-1}^{1} d\phi\,\sqrt{2V(\phi)}\ . \tag{11}$$

Note that, for scalar fields, the two terms in (1) contribute equally to the wall energy.

The profile function $\phi(g)$ has a sigmoid shape (like a hyperbolic tangent). For $g \to \pm\infty$, linearizing (10) around $\phi = \pm 1$ gives

$$1 \mp \phi \sim \exp(-[V''(\pm 1)]^{1/2}|g|) \ , \quad g \to \pm\infty \ , \tag{12}$$

i.e. the order parameter saturates exponentially fast away from the walls. It follows that the excess energy is localized in the domain walls, and that the driving force for the domain growth is the wall curvature, since the system energy can only decrease through a reduction in the total wall area. The growth mechanism is rather different, however, for conserved and nonconserved fields.

2.1.3 The Interface Equation: Nonconserved Fields

The existence of a surface tension implies a force per unit area, proportional to the mean curvature, acting at each point on the wall. The calculation is similar to that of the excess pressure inside a bubble. Consider, for example, a spherical domain of radius R, in three dimensions. If the force per unit area is F, the work done by the force in decreasing the radius by dR is $4\pi F R^2 dR$. Equating this to the decrease in surface energy, $8\pi\sigma R dR$, gives $F = 2\sigma/R$. For model A dynamics, this force will cause the walls to move, with a velocity proportional to the local curvature. If the friction constant for domain-wall motion is η, then this argument gives $\eta\, dR/dt = -2\sigma/R$. For general dimension d, the factor '2' on the right is replaced by $(d-1)$.

It is interesting to see how this result arises directly from the equation of motion (2). We consider a single spherical domain of (say) $\phi = -1$ immersed in a sea of $\phi = +1$. Exploiting the spherical symmetry, (2) reads

$$\frac{\partial\phi}{\partial t} = \frac{\partial^2\phi}{\partial r^2} + \frac{d-1}{r}\frac{\partial\phi}{\partial r} - V'(\phi) \ . \tag{13}$$

Provided the droplet radius R is much larger than the interface width ξ, we expect a solution of the form

$$\phi(r,t) = f\left(r - R(t)\right) \ . \tag{14}$$

Inserting this in (13) gives

$$0 = f'' + [(d-1)/r + dR/dt]f' - V'(f) \ . \tag{15}$$

The function $f(x)$ changes from -1 to 1 in a small region of width ξ near $x = 0$. It's derivative is, therefore, sharply peaked near $x = 0$ (i.e. near $r = R(t)$). Multiplying (15) by f' and integrating through the interface gives

$$0 = (d-1)/R + dR/dt \ , \tag{16}$$

where we have used $f' = 0$ far from the interface, and $V(f)$ has the same value on both sides of the interface (in the absence of a bulk driving force, i.e. a magnetic field). Integrating (16) gives $R^2(t) = R^2(0) - 2(d-1)t$, i.e. the collapse time scales with the initial radius as $t \sim R^2(0)$. Equation (16) is identical to our previous result obtained by considering the surface tension as the driving force, provided the surface tension σ and friction constant η are equal. This we show explicitly below.

The result for general curved surfaces was derived by Allen and Cahn [20], who noted that, close to a domain wall, one can write $\nabla\phi = (\partial\phi/\partial g)_t\, \hat{g}$, where $\hat{g}$ is a unit vector normal to the wall (in the direction of increasing ϕ), and so $\nabla^2\phi = (\partial^2\phi/\partial g^2)_t + (\partial\phi/\partial g)_t\, \nabla\cdot\hat{g}$. Noting also the relation $(\partial\phi/\partial t)_g = -(\partial\phi/\partial g)_t\, (\partial g/\partial t)_\phi$, (2) can be recast as

$$-(\partial\phi/\partial g)_t\, (\partial g/\partial t)_\phi = (\partial\phi/\partial g)_t\, \nabla\cdot\hat{g} + (\partial^2\phi/\partial g^2)_t - V'(\phi) \ . \tag{17}$$

Assuming that, for gently curving walls, the wall profile is given by the equilibrium condition (10), the final two terms in (17) cancel. Noting also that $(\partial g/\partial t)_\phi$ is just the wall velocity v (in the direction of increasing ϕ), (17) simplifies to

$$v = -\nabla \cdot \hat{g} = -K \ , \tag{18}$$

the 'Allen-Cahn equation', where $K \equiv \nabla \cdot \hat{g}$ is $(d-1)$ times the mean curvature. For brevity, we will call K simply the 'curvature'. An alternative derivation of (18) follows the approach used for the spherical domain, i.e. we multiply Eq. (17) by $(\partial\phi/\partial g)_t$ and integrate (with respect to g) through the interface. This gives the same result.

Equation (18) is an important result, because it establishes that the motion of the domain walls is determined (for non-conserved fields) purely by the local curvature. In particular, the detailed shape of the potential is not important: the main role of the double-well potential $V(\phi)$ is to establish (and maintain) well-defined domain walls. (Of course, the well depths must be equal, or there would be a volume driving force).

For a spherical domain, the curvature K is $(d-1)/R$, and (18) reduces to (16). Our explicit treatment of the spherical domain verifies the Allen-Cahn result, and, in particular, the independence from the potential of the interface dynamics.

A second feature of (18) is that the surface tension σ (which *does* depend on the potential) does not explicitly appear. How can this be, if the driving force on the walls contains a factor σ? The reason, as we have already noted, is that one also needs to consider the *friction constant* per unit area of wall, η: The equation of motion for the walls in this dissipative system is $\eta v = -\sigma K$. Consistency with (18) requires $\eta = \sigma$. In fact, η can be calculated independently, as follows. Consider a plane wall moving uniformly (under the influence of some external driving force) at speed v. The rate of energy dissipation per unit area is

$$\begin{aligned} dE/dt &= \int_{-\infty}^{\infty} dg \, \frac{\delta F}{\delta \phi} \frac{\partial \phi}{\partial t} \\ &= -\int_{-\infty}^{\infty} dg \left(\frac{\partial \phi}{\partial t} \right)^2 \ , \end{aligned} \tag{19}$$

using (2). The wall profile has the form $\phi(g,t) = f(g-vt)$, where the profile function f will, in general, depend on v. Putting this form into (19) gives

$$dE/dt = -v^2 \int dg \, (\partial\phi/\partial g)^2 = -\sigma v^2 \ , \tag{20}$$

where the definition (11) of the surface tension σ was used in the final step, and the profile function $f(x)$ replaced by its $v = 0$ form to lowest order in v. By definition, however, the rate of energy dissipation is the product of the frictional force ηv and the velocity, $dE/dt = -\eta v^2$. Comparison with (20) gives $\eta = \sigma$. We conclude that, notwithstanding some contrary suggestions in the literature, the Allen-Cahn equation is completely consistent with the idea that domain growth is driven by the surface tension of the walls.

2.1.4 Conserved Fields

For conserved fields the interfaces cannot move independently. At late times the dominant growth mechanism is the transport of the order parameter from interfaces of high curvature to regions of low curvature by diffusion through the intervening bulk phases. To see how this works, we first linearize (3) in one of the bulk phases, with say $\phi \simeq 1$. Putting $\phi = 1 + \tilde{\phi}$ in (3), and linearizing in $\tilde{\phi}$, gives

$$\partial\tilde{\phi}/\partial t = -\nabla^4\tilde{\phi} + V''(1)\nabla^2\tilde{\phi} \ . \tag{21}$$

Since the characteristic length scales are large at late times, the ∇^4 term is negligible, and (21) reduces to the diffusion equation, with diffusion constant $D = V''(1)$. The interfaces provide the boundary conditions, as we shall see. However, we can first make a further simplification. Due to the conservation law, the interfaces move little during the time it takes the diffusion field $\tilde{\phi}$ to relax. If the characteristic domain size is L, the diffusion field relaxes on a time scale $t_D \sim L^2$. We shall see below, however, that a typical interface velocity is of order $1/L^2$, so the interfaces only move a distance of order unity (i.e. much less than L) in the time t_D. This means that the diffusion field relaxes quickly compared to the rate at which the interfaces move, and is essentially always in equilibrium with the interfaces. The upshot is that the diffusion equation can be replaced by Laplace's equation, $\nabla^2\tilde{\phi} = 0$, in the bulk.

To derive the boundary conditions at the interfaces, it is convenient to work, not with $\tilde{\phi}$ directly, but with the chemical potential $\mu \equiv \delta F/\delta\phi$. In terms of μ, (3) can be written as a continuity equation,

$$\begin{aligned} \partial\phi/\partial t &= -\nabla \cdot j & (22)\\ j &= -\nabla\mu & (23)\\ \mu &= V'(\phi) - \nabla^2\phi\ . & (24) \end{aligned}$$

In the bulk, μ and $\tilde{\phi}$ are proportional to each other, because (24) can be linearized to give $\mu = V''(1)\tilde{\phi} - \nabla^2\tilde{\phi}$, and the ∇^2 term is again negligible. Therefore μ also obeys Laplace's equation,

$$\nabla^2\mu = 0\ , \qquad (25)$$

in the bulk.

The boundary conditions are derived by analysing (24) near an interface. As in the derivation of the Allen-Cahn equation, we consider surfaces of constant ϕ near the interface and introduce a Cartesian coordinate system at each point, with a coordinate g normal to the surface (and increasing with increasing ϕ). Then (24) becomes (compare Eq. (17),

$$\mu = V'(\phi) - (\partial\phi/\partial g)_t\, K - (\partial^2\phi/\partial g^2)_t \qquad (26)$$

near the interface, where $K = \nabla \cdot \hat{g}$ is the curvature. The value of μ at the interface can be obtained (just as in our treatment of the spherical domain in section 2.1.3), by multiplying through by $(\partial\phi/\partial g)_t$, which is sharply peaked at the interface, and integrating over g through the interface. Noting that μ and K vary smoothly through the interface, this gives the completely general relation

$$\mu\Delta\phi = \Delta V - \sigma K \qquad (27)$$

at the interface, where $\Delta\phi$ is the change in ϕ across the interface, and ΔV is the difference in the minima of the potential for the two bulk phases. In deriving (27), we have used $(\partial\phi/\partial g)_t \to 0$ far from the interface, and made the identification $\int dg(\partial\phi/\partial g)_t^2 = \sigma$, as in (11), with σ the surface tension. Simplifying to the case where the minima have equal depth (we shall see that the general case introduces no new physics), and taking the minima to be at $\phi = \pm 1$ as usual, gives $\Delta V = 0$ and $\Delta\phi = 2$. Then (27) becomes

$$\mu = -\sigma K/2\ . \qquad (28)$$

This (or, more generally, Eq. (27)) is usually known as the Gibbs-Thomson boundary condition. Note that we have assumed that the order parameter takes its equilibrium value (± 1) in both bulk phases. This is appropriate to the late stages of growth in which we are primarily interested.

To summarize, (28) determines μ on the interfaces in terms of the curvature. Between the interfaces, μ satisfies the Laplace equation (25). The final step is to

use (23) to determine the motion of the interfaces. An interface moves with a velocity given by the imbalance between the current flowing into and out of it:

$$v\,\Delta\phi = j_{\rm out} - j_{\rm in} = -[\partial\mu/\partial g] = -[\hat{g}\cdot\nabla\mu]\ , \tag{29}$$

where v is the speed of the interface in the direction of increasing ϕ, g is the usual coordinate normal to interface, $[\cdots]$ indicates the discontinuity across the interface, and we have assumed as usual that $\phi \simeq \pm 1$ in the bulk phases.

To illustrate how (25), (28) and (29) are used, we consider again the case of a single spherical domain of negative phase ($\phi = -1$) in an infinite sea of positive phase ($\phi = +1$). We restrict ourselves to $d = 3$ for simplicity. The definition of μ, Eq. (24), gives $\mu = 0$ at infinity. Let the domain have radius $R(t)$. The solution of (25) that obeys the boundary conditions $\mu = 0$ at infinity and (28) at $r = R$, and respects the spherical symmetry is (using $K = 2/R$ for $d = 3$) $\mu = -\sigma/r$ for $r \geq R$. Inside the domain, the $1/r$ term must be absent to avoid an unphysical singularity at $r = 0$. The solution of (25) in this region is therefore $\mu = {\rm const}$. The boundary condition (28) gives $\mu = -\sigma/R$.

To summarize,

$$\begin{aligned} \mu &= -\sigma/R\ , \qquad r \leq R \\ &= -\sigma/r\ , \qquad r \geq R\ . \end{aligned} \tag{30}$$

Using (29), with $\Delta\phi = 2$, then gives

$$dR/dt = v = -\frac{1}{2}[\partial\mu/\partial r]_{R-\epsilon}^{R+\epsilon} = -\sigma/2R^2\ , \tag{31}$$

and hence $R^3(t) = R^3(0) - 3\sigma t/2$. We conclude that a domain of initial radius $R(0)$ evaporates in a time proportional to $R^3(0)$. This contrasts with the $R^2(0)$ result obtained for a non-conserved order parameter. In the non-conserved case, of course, the domain simply shrinks under the curvature forces, whereas for the conserved case it evaporates by the diffusion of material to infinity.

2.1.5 Growth Laws

The scaling hypothesis suggests a simple intuitive derivation of the 'growth laws' for $L(t)$, which are really just generalizations of the calculations for isolated spherical domains. For model A, we can estimate both sides of the Allen-Cahn equation (18) as follows. If there is a single characteristic scale L, then the wall velocity $v \sim dL/dt$, and the curvature $K \sim 1/L$. Equating and integrating gives $L(t) \sim t^{1/2}$ for non-conserved scalar fields.

For conserved fields (model B), the argument is slightly more subtle. We shall follow the approach of Huse [21]. From (28), the chemical potential has a typical value $\mu \sim \sigma/L$ on interfaces, and varies over a length scale of order L. The current, and therefore the interface velocity v, scale as $\nabla\mu \sim \sigma/L^2$, giving $dL/dt \sim \sigma/L^2$ and $L(t) \sim (\sigma t)^{1/3}$. A more compelling argument for this result can be found in [23, 24, 1]. We note, however, that the result is supported by evidence from computer simulations [21, 22] (which usually require , however, some extrapolation into the asymptotic scaling regime) as well as a Renormalization Group (RG) treatment [5, 6]. In the limit that one phase occupies an infinitesimal volume fraction, the original Lifshitz-Slyozov-Wagner theory convincingly demonstrates a $t^{1/3}$ growth. This calculation, whose physical mechanism is the evaporation of material (or magnetization) from small droplets and condensation onto larger droplets, will be discussed briefly in the following subsection.

It is interesting that these growth laws can also be obtained using naive arguments based on the results for single spherical domains [3]. For nonconserved dynamics, we know that a domain of radius R collapses in a time of order R^2. Therefore, crudely speaking, after time t there will be no domains smaller than $t^{1/2}$,

so the characteristic domain size is $L(t) \sim t^{1/2}$. Of course, this is an oversimplification, but it captures the essential physics. For conserved dynamics, the same line of argument leads to $t^{1/3}$ growth. In fact, this approach can be used rather generally, for a variety of systems, and gives results which agree, in nearly all cases, with the exact growth laws [23, 24, 1]

2.2 Topological Defects

The domain walls discussed in the previous section are the simplest form of 'topological defect', and occur in systems described by scalar fields [25]. They are surfaces, on which the order parameter vanishes, separating domains of the two equilibrium phases. A domain wall is topologically stable: local changes in the order parameter can move the wall, but cannot destroy it. For an isolated flat wall, the wall profile function is given by the solution of (10), with the appropriate boundary conditions, as discussed in section 2.1.2. For the curved walls present in the phase ordering process, this will still be an approximate solution locally, provided the typical radius of curvature L is large compared to the intrinsic width (or 'core size'), ξ, of the walls. (This could be defined from (12) as $\xi = [V''(1)]^{-1/2}$, say). The same condition, $L \gg \xi$, ensures that typical wall separations are large compared to their width.

Let us now generalize the discussion to vector fields. The '$O(n)$ model' is described by an n-component vector field $\vec{\phi}(\mathbf{x}, t)$, with a free energy functional $F[\vec{\phi}]$ that is invariant under global rotations of $\vec{\phi}$. A suitable generalization of (1) is

$$F[\vec{\phi}] = \int d^d x \left(\frac{1}{2} (\nabla \vec{\phi})^2 + V(\vec{\phi}) \right) , \tag{32}$$

where $(\nabla \vec{\phi})^2$ means $\sum_{i=1}^{d} \sum_{a=1}^{n} (\partial_i \phi^a)^2$ (i.e. a scalar product over both spatial and 'internal' coordinates), and $V(\vec{\phi})$ is 'mexican hat' (or 'wine bottle') potential, such as $(1-\vec{\phi}^2)^2$. It is clear that $F[\vec{\phi}]$ is invariant under global rotations of $\vec{\phi}$ (a continuous symmetry), rather than just the inversion symmetry ($\phi \to -\phi$, a discrete symmetry) of the scalar theory. We will adopt the convention that V has its minimum for $\vec{\phi}^2 = 1$.

For non-conserved fields, the simplest dynamics (model A) is a straightforward generalization of (2), namely

$$\partial \vec{\phi} / \partial t = \nabla^2 \vec{\phi} - dV/d\vec{\phi} \, . \tag{33}$$

For conserved fields (model B), we simply add another $(-\nabla^2)$ in front of the right-hand side.

Stable topological defects for vector fields can be generated, in analogy to the scalar case, by seeking stationary solutions of (33) with appropriate boundary conditions. For the $O(n)$ theory in d-dimensional space, the requirement that all n components of $\vec{\phi}$ vanish at the defect core defines a surface of dimension $d - n$ (e.g. a domain wall is a surface of dimension $d - 1$: the scalar theory corresponds to $n = 1$). The existence of such defects therefore requires $n \leq d$. For $n = 2$ these defects are points ('vortices') for $d = 2$ or lines ('strings', or 'vortex lines') for $d = 3$. For $n = 3$, $d = 3$ they are points ('hedgehogs', or 'monopoles'). The field configurations for these defects are sketched in Figures 3(a)-(d). Note that the forms shown are radially symmetric with respect to the defect core: any configuration obtained by a global rotation is also acceptable. For $n < d$, the field $\vec{\phi}$ only varies in the n dimensions 'orthogonal' to the defect core, and is uniform in the remaining $d - n$ dimensions 'parallel' to the core.

For $n < d$, the defects are spatially extended. Coarsening occurs by a 'straightening out' (or reduction in typical radius of curvature) as sharp features are removed, and by the shrinking and disappearance of small domain bubbles or vortex loops. These processes reduce the total area of domain walls, or length of vortex line, in the system. For point defects ($n = d$), coarsening occurs by the mutual annihilation

of defect-antidefect pairs. The antidefect for a vortex ('antivortex') is sketched in Figure 3(e). Note that the antivortex in *not* obtained by simply reversing the directions of the arrows in 10(b): this would correspond to a global rotation through π. Rather, the vortex and antivortex have different 'topological charges': the fields rotates by 2π or -2π respectively on encircling the defect. By contrast, an antimonopole *is* generated by reversing the arrows in 10(d): the reversed configuration cannot be generated by a simple rotation in this case.

For the radially symmetric defects illustrated in 10(b)–(d), the field $\vec{\phi}$ has the form $\vec{\phi}(\mathbf{r}) = \hat{r}\, f(r)$, where $\hat{r}$ is a unit vector in the radial direction, and $f(r)$ is the profile function. Inserting this form into (33), with the time derivative set to zero, gives the equation

$$\frac{d^2 f}{dr^2} + \frac{(n-1)}{r}\frac{df}{dr} - \frac{(n-1)}{r^2} f - V'(f) = 0 \ , \tag{34}$$

with boundary conditions $f(0) = 0$, $f(\infty) = 1$. Of special interest is the approach to saturation at large r. Putting $f(r) = 1 - \epsilon(r)$ in (34), and expanding to first order in ϵ, yields

$$\epsilon(r) \simeq \frac{(n-1)}{V''(1)}\frac{1}{r^2} \ , \qquad r \to \infty \ . \tag{35}$$

This should be contrasted with the exponential approach to saturation (12) for scalar fields. A convenient definition of the 'core size' ξ is through $f \simeq 1 - \xi^2/r^2$ for large r. This gives $\xi = [(n-1)/V''(1)]^{1/2}$ for $n > 1$.

2.2.1 Defects Energetics

Consider an isolated, equilibrium defect of the $O(n)$ model in d-dimensional space (with, of course, $n \leq d$). For a radially symmetric defect, $\vec{\phi}(\mathbf{r}) = f(r)\,\hat{\mathbf{r}}$, the energy per unit 'core volume' (e.g. per unit area for a wall, per unit length for a line, or per defect for a point) is, from (32)

$$E = S_n \int dr\, r^{n-1} \left(\frac{(n-1)}{2r^2} f^2 + \frac{1}{2}(\nabla f)^2 + V(f) \right) \ , \tag{36}$$

where $S_n = 2\pi^{n/2}/\Gamma(n/2)$ is the surface area of an n-dimensional sphere.

For scalar fields ($n = 1$), we have seen (section 2.1.2) that the terms in $(\nabla f)^2$ and $V(f)$ contribute equally to the wall energy. For $n \geq 2$, the first term in (36) dominates the other two because, from (35), the three terms in the integrand fall off with distance as r^{-2}, r^{-6} and $V(f) \sim V''(1)(1-f)^2 \sim r^{-4}$ respectively as $r \to \infty$. For $n \geq 2$, therefore, the first term gives a divergent integral which has to be cut off as the system size L_{sys}, i.e. $E \sim \ln(L_{sys}/\xi)$ for $n = 2$ and $E \sim L_{sys}^{n-2}$ for $n > 2$. Actually, the second and third terms give divergent integrals for $n \geq 6$ and $n \geq 4$ respectively, but these are always subdominant compared to the first term.

The above discussion concerns an *isolated* defect. In the phase ordering system the natural cut-off is not L_{sys} but $L(t)$, the characteristic scale beyond which the field of a single defect will be screened by the other defects. Of particular interest are the dynamics of defect structures much smaller than $L(t)$. These are the analogues of the small domains of the scalar system. For $d = n = 2$, these are vortex-antivortex pairs, for $d = 3$, $n = 2$ they are vortex rings, while for $d = 3 = n$ they are monopole-antimonopole pairs. For such a structure, the pair separation r (for point defects) or ring radius r (for a vortex loop) provide the natural cut-off. Including the factor r^{d-n} for the volume of defect core, the energy of such a structure is

$$\begin{aligned} E &\sim r^{d-2} \ln(r/\xi) \ , \qquad d \geq n = 2 \ , \\ &\sim r^{d-2} \ , \qquad\quad d \geq n > 2 \ . \end{aligned} \tag{37}$$

The derivative with respect to r of this energy provides the driving force, $-dE/dr$, for the collapse of the structure. Dividing by r^{d-n} gives the force F acting on a unit volume of core (i.e. per unit length for strings, per point for points, etc.):

$$\begin{aligned} F(r) &\sim -r^{-1} , & d = n = 2 , \\ &\sim -r^{n-3} \ln(r/\xi) , & d > n = 2 , \\ &\sim -r^{n-3} , & d \geq n > 2 . \end{aligned} \tag{38}$$

In order to calculate the collapse time we need the analogue of the 'friction constant' η (see section 2.1.3) for vector fields. This we calculate in the next section. Before doing so, we compute the total energy density ϵ for vector fields. This can be obtained by putting $r \sim L(t)$ in (37), and dividing by a characteristic volume $L(t)^d$ (since there will typically be of order one defect structure, with size of order $L(t)$, per scale volume $L(t)^d$),

$$\begin{aligned} \epsilon &\sim L(t)^{-2} \ln(L(t)/\xi) , & d \geq n = 2 , \\ &\sim L(t)^{-2} , & d \geq n > 2 . \end{aligned} \tag{39}$$

For scalar systems, of course, $\epsilon \sim L(t)^{-1}$.

As a caveat to the above discussion, we note that we have explicitly assumed that the individual defects possess an approximate radial symmetry on scales small compared to $L(t)$. It has been known for some time [26], however, that an isolated point defect for $d > 3$ can lower its energy by having the field uniform (pointing 'left', say) over most of space , with a narrow 'flux tube' of field in the opposite direction (i.e. pointing 'right'). The energy is then linear in the size of the system, $E \sim L_{sys}\xi^{d-3}$, which is smaller than the energy, $\sim L_{sys}^{d-2}$, of the spherically symmetric defect, for $d > 3$. A defect-antidefect pair with separation r, connected by such a flux tube, has an energy $E \sim r\xi^{d-3}$, which implies an r-independent force for all $d \geq 3$, in contrast to (38).

How relevant are these considerations in the context of phase-ordering dynamics? These single-defect and defect-pair calculations treat the field as completely relaxed with respect to the defect cores. If this were true we could estimate the energy density for typical defect spacing $L(t)$ as $\xi^{d-3}L(t)^{1-d}$ for $d > 3$. However, the smooth variation ('spin waves') of the field between the defects gives a contribution to the energy density of $(\nabla\phi)^2 \sim L(t)^{-2}$, which dominates over the putative defect contribution for $d > 3$. Under these circumstances, we would not expect a strong driving force for point defects to adopt the 'flux tube' configuration, since the energy is dominated by spin waves. Rather, our tentative picture is of the point defects 'riding' on the evolving spin wave structure for $d > 3$, although this clearly requires further work. Note, however, that these concerns are only relevant for $d > 3$: Eq. (38) is certainly correct for the physically relevant cases $d \leq 3$.

2.2.2 Defect Dynamics

Here we will consider only nonconserved fields, although it is possible to generalize the results to conserved fields [24]. The caveats for $d > 3$ discussed in the previous subsection also apply here.

The calculation of the friction constant η proceeds as in section 2.1.3. Consider an isolated equilibrium defect, i.e. a vortex for $d = n = 2$, a monopole for $n = d = 3$, a straight vortex line for $n = 2$, $d = 3$ etc. Set up a Cartesian coordinate system $x_1, \ldots, x_d$. For extended defects, let the defect occupy the (hyper)-plane defined by the last $d - n$ Cartesian coordinates, and move with speed v in the x_1 direction. Then $\vec{\phi}$ only depends on coordinates $x_1, \ldots, x_n$, and the rate of change of the system energy per unit volume of defect core is

$$\begin{aligned} dE/dt &= \int dx_1 \ldots dx_n \, (\delta F/\delta\vec{\phi}) \cdot \partial\vec{\phi}/\partial t \\ &= -\int dx_1 \ldots dx_n \, (\partial\vec{\phi}/\partial t)^2 . \end{aligned} \tag{40}$$

The defect profile has the form $\vec{\phi}(x_1,\ldots,x_n) = \vec{f}(x_1 - vt, x_2, \ldots, x_n)$, where the function $\vec{f}$ depends on v in general. Putting this into (40) gives

$$\begin{aligned} dE/dt &= -v^2 \int dx_1 \ldots dx_n \, (\partial\vec{\phi}/\partial x_1)^2 \\ &= -(v^2/n) \int d^n r (\nabla\vec{\phi})^2 = -\eta v^2 \,, \end{aligned} \tag{41}$$

where the function $\vec{f}$ has been replace by its $v = 0$ form to lowest order in v, and η is the friction constant per unit core volume. The final expression follows from symmetry. It follows that η is (up to constants) equal to the defect energy per unit core volume. In particular, it diverges with the system size for $n \geq 2$. For a small defect structure of size r, we expect the divergence to be effectively cut off at r. This gives a scale-dependent friction constant,

$$\begin{aligned} \eta(r) &\sim r^{n-2} \ln(r/\xi) \,, \qquad d \geq n = 2 \,, \\ &\sim r^{n-2} \,, \qquad\quad d \geq n > 2 \,. \end{aligned} \tag{42}$$

Invoking the scaling hypothesis, we can now determine the growth laws for non-conserved vector systems. Eqs. (38) and (42) give the typical force and friction constant per unit core volume as $F(L)$ and $\eta(L)$. Then a typical velocity is $v \sim dL/dt \sim F(L)/\eta(L)$, which can be integrated to give, asymptotically,

$$\begin{aligned} L(t) &\sim (t/\ln t)^{1/2} \,, \qquad d = n = 2 \,, \\ &\sim t^{1/2} \,, \qquad \text{otherwise} \,. \end{aligned} \tag{43}$$

The result for $n = d = 2$ was derived by Pargellis et al. [27], and checked numerically by Yurke et al. [28]. The method used here follows their approach [29]. The key concept of a scale-dependent friction constant has been discussed by a number of authors [30]. A detailed analysis of monopole-antimonopole annihilation, in the context of nematic liquid crystals, has been given by Pismen and Rubinstein [31].

A more general and powerful method to derive growth laws, valid for both conserved and nonconserved systems, has been given elsewhere [23, 24, 1]. The results agree with the intuitive arguments presented above.

2.2.3 Porod's Law

The presence of topological defects, seeded by the initial conditions, in the system undergoing phase ordering has an important effect on the 'short-distance' form of the pair correlation function $C(\mathbf{r},t)$, and therefore on the 'large-momentum' form of the structure factor $S(\mathbf{k},t)$. To see why this is so, we note that, according to the scaling hypothesis, we would expect a typical field gradient to be of order $|\nabla\vec{\phi}| \sim 1/L$. At a distance r from a defect core, however, with $\xi \ll r \ll L$, the field gradient is much larger, of order $1/r$ (for a vector field), because $\vec{\phi} = \hat{r}$ implies $(\nabla\vec{\phi})^2 = (n-1)/r^2$. Note that we require $r \gg \xi$ for the field to be saturated, and $r \ll L$ for the defect field to be largely unaffected by other defects (which are typically a distance L away). This gives a meaning to 'short' distances ($\xi \ll r \ll L$), and 'large momenta' ($L^{-1} \ll k \ll \xi^{-1}$). The large field gradients near defects leads to a non-analytic behaviour at $x = 0$ of the scaling function $f(x)$ for pair correlations.

We start by considering scalar fields. Consider two points $\mathbf{x}$ and $\mathbf{x}+\mathbf{r}$, with $\xi \ll r \ll L$. The product $\phi(\mathbf{x})\,\phi(\mathbf{x}+\mathbf{r})$ will be -1 if a wall passes between them, and $+1$ if there is no wall. Since $r \ll L$, the probability to find more than one wall can be neglected. The calculation amounts to finding the probability that a randomly placed rod of length r cuts a domain wall. This probability is of order r/L, so we estimate

$$\begin{aligned} C(\mathbf{r},t) &\simeq (-1) \times (r/L) + (+1) \times (1 - r/L) \\ &= 1 - 2r/L \,, \qquad r \ll L \,. \end{aligned} \tag{44}$$

The factor 2 in this result should not be taken seriously.

The important result is that (44) is non-analytic in $\mathbf{r}$ at $\mathbf{r} = 0$, since it is linear in $r \equiv |\mathbf{r}|$. Technically, of course, this form breaks down inside the core region, when $r < \xi$. We are interested, however, in the scaling limit defined by $r \gg \xi$, $L \gg \xi$, with $x = r/L$ arbitrary. The nonanalyticity is really in the scaling variable x.

The nonanalytic form (44) implies a power-law tail in the structure factor, which can be obtained from (44) by simple power-counting:

$$S(\mathbf{k}, t) \sim \frac{1}{L\, k^{d+1}} , \qquad kL \gg 1 , \tag{45}$$

a result known universally as 'Porod's law'. It was first written down in the general context of scattering from two-phase media [18]. Again, one requires $k\xi \ll 1$ for the scaling regime. Although the k-dependence of (45) is what is usually referred to as Porod's law, the L-dependence is equally interesting. The factor $1/L$ is simply (up to constants) the total area of domain wall per unit volume, a fact appreciated by Porod, who proposed structure factor measurements as a technique to determine the area of interface in a two-phase medium [18]. On reflection, the factor $1/L$ is not so surprising. For $kL \gg 1$, the scattering function is probing structure on scales much shorter than the typical interwall spacing or radius of curvature. In this regime we would expect the structure factor to scale as the total wall area, since each element of wall with linear dimension large compared to $1/k$ contributes essentially independently to the structure factor.

This observation provides the clue to how to generalize (45) to vector (and other) fields [32, 33]. The idea is that, for $kL \gg 1$, the structure factor should scale as the total volume of defect core. Since the dimension of the defects is $d - n$, the amount of defect per unit volume scales as L^{-n}. Extracting this factor from the general scaling form (7) yields

$$S(\mathbf{k}, t) \sim \frac{1}{L^n\, k^{d+n}} , \qquad kL \gg 1 , \tag{46}$$

for the $O(n)$ theory, a 'generalized Porod's law'.

Equation (46) was first derived from approximate treatments of the equation of motion (33) for nonconserved fields [34, 35, 36, 37]. In these derivations, however, the key role of topological defects was far from transparent. The above heuristic derivation suggests that the result is in fact very general (e.g., it should hold equally well for conserved fields), with extensions beyond simple $O(n)$ models. The appropriate techniques, which also enable the amplitude of the tail to be determined, were developed by Bray and Humayun [33].

2.3 Scaling Functions

We begin by discussing phase ordering of a vector field in the limit that the number of vector components of the field, n, tends to infinity. This limit has been studied, mostly for nonconserved fields, by a large number of authors [12, 16, 38, 39, 40, 41]. In principle, the solution is the starting point for a systematic treatment in powers of $1/n$. In practice, the calculation of the $O(1/n)$ terms is technically difficult [16, 41]. Moreover, some important physics is lost in this limit. In particular, there are no topological defects, since clearly $n > d + 1$ for any d as $n \to \infty$. As a consequence, Porod's law (46), for example, is not found. It turns out, however, that similar techniques can be applied for any n after a preliminary transformation from the physical order parameter field $\vec{\phi}$ to a suitably chosen 'auxiliary field' $\vec{m}$. This is discussed in sections 2.3.3 and 2.3.5. The topological defects are incorporated through the functional dependence of $\vec{\phi}$ on $\vec{m}$, and Porod's law is recovered.

2.3.1 The Large-n Limit: Nonconserved Fields

Although not strictly necessary, it is convenient to choose in (33) the familiar 'ϕ^4' potential, in the form $V(\vec{\phi}) = (n - \vec{\phi}^2)^2/4n$, where the explicit n-dependence is for later convenience in taking the limit $n \to \infty$. With this potential, (33) becomes

$$\partial\vec{\phi}/\partial t = \nabla^2\vec{\phi} + \vec{\phi} - \frac{1}{n}(\vec{\phi}^2)\,\vec{\phi}\,. \tag{47}$$

The simplest way to take the limit is to recognize that, for $n \to \infty$, $\vec{\phi}^2/n$ can be replaced by its average, to give

$$\partial\phi/\partial t = \nabla^2\phi + a(t)\,\phi \tag{48}$$

$$a(t) = 1 - \langle\phi^2\rangle\,, \tag{49}$$

where ϕ now stands for (any) one of the components of $\vec{\phi}$. Eq. (48) can alternatively be derived by standard diagrammatic techniques [16]. Eq. (48) can be solved exactly for arbitrary time t after the quench. However, we are mainly interested in late times (i.e. the scaling regime), when the solution simplifies. After Fourier transformation, the formal solution of (48) is

$$\phi_{\mathbf{k}}(t) = \phi_{\mathbf{k}}(0)\,\exp[-k^2t + b(t)]\,, \tag{50}$$

$$b(t) = \int_0^t dt'\,a(t')\,, \tag{51}$$

giving

$$a(t) = db/dt = 1 - \Delta\sum_k \exp[-2k^2t + 2b(t)]\,, \tag{52}$$

where (4) has been used to eliminate the initial condition. Since we shall find *a posteriori* that $a(t) \ll 1$ at late times, the left side of (52) is negligible for $t \to \infty$. Using $\sum_{\mathbf{k}} \exp(-2k^2t) = (8\pi t)^{-d/2}$ gives $b(t) \to (d/4)\ln(t/t_0)$, where

$$t_0 = \Delta^{2/d}/8\pi\,. \tag{53}$$

Therefore, $a(t) \to d/4t$ for $t \to \infty$, and the solution of (50), valid at late times, is

$$\phi_{\mathbf{k}}(t) = \phi_{\mathbf{k}}(0)\,(t/t_0)^{d/4}\,\exp(-k^2t)\,. \tag{54}$$

Using (4) once more, we obtain the structure factor, and its Fourier transform, the pair correlation function as,

$$S(\mathbf{k},t) = (8\pi t)^{d/2}\,\exp(-2k^2t)\,, \tag{55}$$

$$C(\mathbf{r},t) = \exp(-r^2/8t)\,. \tag{56}$$

These results exhibit the expected scaling forms (7), with length scale $L(t) \propto t^{1/2}$. Note that the structure factor has a gaussian tail, in contrast to the power-law tail (46) found in systems with $n \leq d$. It might be hoped, however, that the large-n forms (55) and (56) would be qualitatively correct in systems with no topological defects, i.e. for $n > d + 1$.

2.3.2 Two-Time Correlations

Within the large-n solution, we can also calculate two-time correlations to test the scaling form (8). It turns out (although this becomes apparent only at $O(1/n)$) [16, 41] that there is a new, non-trivial, exponent associated with the limit when the two times are well separated [42].

From (54) it follows immediately that

$$S(\mathrm{k},t,t') \equiv \langle \phi_{\mathrm{k}}(t)\phi_{-\mathrm{k}}(t')\rangle = [8\pi(tt')^{1/2}]^{d/2}\,\exp[-k^2(t+t')]\;, \tag{57}$$

$$C(\mathbf{r},t,t') \equiv \langle \phi(\mathbf{r},t)\phi(\mathbf{0},t')\rangle = \left[\frac{4tt'}{(t+t')^2}\right]^{d/4} \exp\left[-\frac{r^2}{4(t+t')}\right]\;. \tag{58}$$

Eq. (58) indeed has the expected form (8). In the limit $t \gg t'$, (58) becomes

$$C(\mathbf{r},t,t') = (4t'/t)^{d/4}\,\exp(-r^2/4t)\;, \tag{59}$$

$$= (L'/L)^{\bar{\lambda}}\,h(r/L)\;, \tag{60}$$

where the last equation defines the exponent $\bar{\lambda}$ through the dependence on the *later* time t. Clearly, $\bar{\lambda} = d/2$ for $n = \infty$. When the $O(1/n)$ correction is included, however, an entirely non-trivial result is obtained [16, 41].

It is interesting to consider the special case where the earlier time t' is zero. Then $C(\mathbf{r},t,0)$ is just the correlation with the initial condition. This quantity is often studied in numerical simulations as a convenient way to determine the exponent $\bar{\lambda}$. Within the large-n solution, Eqs. (54) and (53) give, in Fourier and real space,

$$S(\mathrm{k},t,0) = [8\pi(tt_0)^{1/2}]^{d/2}\,\exp(-k^2t)\;, \tag{61}$$

$$C(\mathbf{r},t,0) = (4t_0/t)^{d/4}\,\exp(-r^2/4t)\;. \tag{62}$$

This is just what one gets by replacing t' by t_0 in (57) and (58) (with t_0 playing the role of a short-time cut-off), and then neglecting t_0 compared to t.

A related function is the *response* to the initial condition, defined by

$$G(\mathrm{k},t) = \langle \partial\phi_{\mathrm{k}}(t)/\partial\phi_{\mathrm{k}}(0)\rangle\;. \tag{63}$$

Within the large-n solution, (54) gives immediately

$$G(\mathrm{k},t) = (t/t_0)^{d/4}\,\exp(-k^2t)\;. \tag{64}$$

Comparing (61) and (64), and using (53) once more gives the relation.

$$S(\mathrm{k},t,0) = \Delta\, G(\mathrm{k},t)\;. \tag{65}$$

In fact, this is an exact result, valid beyond the large-n limit, as may be proved easily using integration by parts on the gaussian distribution for $\{\phi_{\mathrm{k}}(0)\}$. The general scaling form for $G(\mathrm{k},t)$,

$$G(\mathbf{k},t) = L^{\lambda}\,g_R(kL)\;, \tag{66}$$

defines a new exponent λ, equal to $d/2$ for $n = \infty$. Since, however, the correlation with the initial condition has the scaling form $C(\mathbf{r},t,0) = L^{-\bar{\lambda}}\,f(r/L)$, the identity (65) gives immediately [43]

$$\bar{\lambda} = d - \lambda\;. \tag{67}$$

(The symbol λ is also used for the transport coefficient in systems with conserved dynamics. This should not be a source of confusion, as the meaning will be clear from the context).

Before leaving this section, it is interesting to consider to what extent the results depend on the specific form (4) chosen for the correlator of the initial conditions. Let us replace the right-hand side of (4) by a function $\Delta(|\mathrm{x}-\mathrm{x}'|)$, with Fourier transform $\Delta(k)$. Then $\Delta(k)$ will appear inside the sum over k in Eq. (52). The dominant k values in the sum, however, are of order $t^{-1/2}$, so for late times we can replace $\Delta(k)$ by $\Delta(0)$, provided the latter exists. This means that universal results are obtained when only *short-range* spatial correlations are present at $t = 0$. For sufficiently *long-range* correlations however, such that $\Delta(k)$ diverges for $k \to 0$, new universality classes are obtained. A general treatment of long-range correlated initial conditions is given in [44].

2.3.3 The OJK Theory

A common theme, introduced by Ohta, Jasnow, and Kawasaki [45] (OJK), in the approximate theories of scaling functions is the replacement of the physical field $\phi(\mathbf{x},t)$, which is ± 1 everywhere except at domain walls, where it varies rapidly, by an auxiliary field $m(\mathbf{x},t)$, which varies smoothly in space. This is achieved by using a non-linear function $\phi(m)$ with a 'sigmoid' shape (such as $\tanh m$). In the OJK theory, the dynamics of the domain walls themselves, defined by the zeros of m, are considered. The normal velocity of a point on the interface is given by the Allen-Cahn equation (9), $v = -K = -\nabla\cdot\mathbf{n}$, where K is the curvature, and $\mathbf{n} = \nabla m/|\nabla m|$ is a unit vector normal to the wall. This gives

$$v = \{-\nabla^2 m + n_a n_b \nabla_a \nabla_b m\}/|\nabla m| \ . \tag{68}$$

In a frame of reference comoving with the interface,

$$dm/dt = 0 = \partial m/\partial t + \mathbf{v}\cdot\nabla m \ . \tag{69}$$

But since $\mathbf{v}$ is parallel to ∇m (and defined in the same direction), $\mathbf{v}.\nabla m = v|\nabla m|$ so

$$v = -\frac{1}{|\nabla m|}\frac{\partial m}{\partial t} \ . \tag{70}$$

Eliminating v between (68) and (70) gives the OJK equation

$$\partial m/\partial t = \nabla^2 m - n_a n_b \nabla_a \nabla_b m \ . \tag{71}$$

Since $\mathbf{n} = \nabla m/|\nabla m|$, this equation is non-linear. To make further progress, OJK made the simplifying approximation of replacing $n_a n_b$ by its spherical average δ_{ab}/d, obtaining the simple diffusion equation

$$\partial m/\partial t = D\,\nabla^2 m \ , \tag{72}$$

with diffusion constant $D = (d-1)/d$.

Providing there are no long-range correlations present, we do not expect the form of the random initial conditions to play an important role in the late-stage scaling. A convenient choice is a gaussian distribution for the field $m(\mathbf{x},0)$, with mean zero and correlator

$$\langle m(\mathbf{x},0)m(\mathbf{x}',0)\rangle = \Delta\delta(\mathbf{x}-\mathbf{x}') \ . \tag{73}$$

Then the linearity of (72) ensures that the field $m(\mathbf{x},t)$ has a gaussian distribution at all times. Solving (72), and averaging over initial conditions using (73) gives the equal-time correlation function

$$\langle m(1)m(2)\rangle = \frac{\Delta}{(8\pi Dt)^{d/2}}\exp\left(-\frac{r^2}{8Dt}\right) \ , \tag{74}$$

where '1' and '2' represent space points separated by r. Of special relevance in what follows is the normalized correlator

$$\gamma(12) \equiv \frac{\langle m(1)m(2)\rangle}{\langle m(1)^2\rangle^{1/2}\langle m(2)^2\rangle^{1/2}} = \exp\left(-\frac{r^2}{8Dt}\right) \ . \tag{75}$$

The generalization to different times is straightforward [46] and will be given explicitly below.

To calculate the pair correlation function of the original field ϕ, we need to know the joint probability distribution for $m(1)$ and $m(2)$. For a gaussian field this can be expressed in terms of the second moments of m:

$$P\left(m(1),m(2)\right) = N\exp\left(-\frac{1}{2(1-\gamma^2)}\left[\frac{m(1)^2}{S_0(1)} + \frac{m(2)^2}{S_0(2)} - 2\gamma\frac{m(1)m(2)}{\sqrt{S_0(1)S_0(2)}}\right]\right) \ , \tag{76}$$

where $\gamma = \gamma(12)$, and

$$S_0(1) = \langle m(1)^2 \rangle, \quad S_0(2) = \langle m(2)^2 \rangle, \quad N = (2\pi)^{-1}[(1-\gamma^2)S_0(1)S_0(2)]^{-1/2} \ . \quad (77)$$

Note that (76) is a general expression for the joint probability distribution of a gaussian field, with γ defined by the first part of (75). Now '1' and '2' represent arbitrary space-time points. For the special case where m obeys the diffusion equation (72), γ is given by

$$\gamma = \left(\frac{4t_1 t_2}{(t_1+t_2)^2} \right)^{d/4} \exp\left(-\frac{r^2}{4D(t_1+t_2)} \right) \ , \quad (78)$$

a simple generalization of (75).

The pair correlation function is given by $C(\mathbf{r},t) = \langle \phi(m(1))\,\phi(m(2)) \rangle$. In the scaling regime, one can replace the function $\phi(m)$ by $\mathrm{sgn}\,(m)$, because the walls occupy a negligible volume fraction. In a compact notation,

$$C(12) = \langle \mathrm{sgn}\, m(1)\, \mathrm{sgn}\, m(2) \rangle = (2/\pi)\, \sin^{-1}(\gamma) \ . \quad (79)$$

The gaussian average over the field m required in (79) is standard (see, e.g., [47]). Eqs. (75) and (79) define the 'OJK scaling function' for equal-time pair correlations. Note that (apart from the trivial dependence through D) it is independent of the spatial dimension d. We will present arguments that it becomes exact in the large-d limit. The OJK function fits experiment and simulation data very well.

The general two-time correlation function is especially interesting in the limit $t_1 \gg t_2$ that defines (see, e.g., (60)) the exponent $\bar{\lambda}$. Since $\gamma \ll 1$ in this limit, (79) can be linearized in γ to give $C(\mathbf{r}, t_1, t_2) \sim (4t_1/t_2)^{d/4} \exp(-r^2/4Dt_2)$, i.e. $\bar{\lambda} = d/2$ within the OJK approximation.

2.3.4 The KYG Method

An earlier approach, due to Kawasaki, Yalabik and Gunton (KYG) [48], building on still earlier work of Suzuki [53], was based on an approximate resummation of the direct perturbation series in the non-linearity, for the quartic potential $V(\phi) = (1/4)(1-\phi^2)^2$. The equation of motion (2) for this potential is

$$\partial\phi/\partial t = \nabla^2\phi + \phi - g\phi^3 \ , \quad (80)$$

with $g = 1$. The basic idea is treat g as small, expand in powers of g, extract the leading asymptotic (in t) behaviour of each term in the series, and set $g = 1$ at the end. However, an uncontrolled approximation is made in simplifying the momentum dependence of each term (the expansion is performed in Fourier space). After setting $g = 1$, the final result can be expressed in terms of the mapping

$$\phi(m) = m/(1+m^2)^{1/2} \ . \quad (81)$$

It is found that m obeys the equation

$$\partial m/\partial t = \nabla^2 m + m \ , \quad (82)$$

instead of (72), which gives an exponential growth superimposed on the diffusion. After the replacement $\phi(m) \to \mathrm{sgn}(m)$, however, this drops out: the OJK scaling function (79) is recovered, with γ given by (75) (but with $D = 1$).

The nature of the approximation involved can be clarified by putting (81) into (80) (with $g = 1$) to derive the exact equation satisfied by m:

$$\frac{\partial m}{\partial t} = \nabla^2 m + m - 3\,\frac{m(\nabla m)^2}{1+m^2} \ . \quad (83)$$

In contrast to a claim made in [48], there is no reason to neglect the final term. On a physical level, the fact that this approach gives the correct growth law, $L(t) \sim t^{1/2}$, seems to be fortuitous. In particular, the crucial role of the interfacial curvature in driving the growth is not readily apparent in this method. By contrast the OJK approach, while giving the same final result, clearly contains the correct physics.

Despite its shortcomings, the KYG method has the virtue that it can be readily extended to vector fields [34, 54]. Eq. (82) is again obtained, but with m replaced by a vector auxiliary field $\vec{m}$, with $\vec{\phi} = \vec{m}/(1+\vec{m}^2)^{1/2}$. At late times, $\vec{\phi} \to \hat{m}$, a unit vector, almost everywhere and $C(12) = \langle \hat{m}(1) \cdot \hat{m}(2) \rangle$. Taking gaussian initial conditions for $\vec{m}$, the resulting scaling function is [34], with γ again given by (75) (but with $D = 1$),

$$C(12) = \frac{n\gamma}{2\pi} \left[B\left(\frac{n+1}{2}, \frac{1}{2}\right)\right]^2 F\left(\frac{1}{2}, \frac{1}{2}; \frac{n+2}{2}; \gamma^2\right) , \tag{84}$$

where $B(x,y)$ is the beta function and $F(a,b;c;z)$ the hypergeometric function ${}_2F_1$. The same scaling function was obtained independently by Toyoki [35]. We will call it the 'BPT scaling function'. The result (75) for γ implies $L(t) \sim t^{1/2}$ for all n within this approximation.

2.3.5 Mazenko's Method

In an interesting series of papers, Mazenko [49, 50, 51] has introduced a new approach that deals with the interface in a natural way. This approach combines a clever choice for the function $\phi(m)$ with the minimal assumption that the field m is gaussian. Specifically $\phi(m)$ is chosen to be the *equilibrium interface profile function*, defined by (compare Eq. (10))

$$\phi''(m) = V'(\phi) , \tag{85}$$

with boundary conditions $\phi(\pm\infty) = \pm 1$, $\phi(0) = 0$. The field m then has a physical interpretation, near walls, as a coordinate normal to the wall. Note that this mapping transforms a problem with *two* length scales, the domain scale $L(t)$ and the interface width ξ, into one with only a *single* length scale, namely $L(t)$ (see Fig. 4). With the choice (85) for $\phi(m)$, the TDGL equation (2) becomes

$$\partial_t \phi = \nabla^2 \phi - \phi''(m) . \tag{86}$$

Multiplying by ϕ at a different space point and averaging over initial conditions gives

$$(1/2)\partial_t C(12) = \nabla^2 C(12) - \langle \phi''(m(1))\, \phi(m(2)) \rangle . \tag{87}$$

So far this is exact. In order to simplify the final term in (87), Mazenko assumes that m can be treated as a gaussian field. Then the final term can be expressed in terms of $C(12)$ itself as follows, exploiting the Fourier decomposition of $\phi(m)$ and the gaussian property of m [50]:

$$\begin{aligned} \langle \phi''(m(1))\, \phi(m(2)) \rangle &= \sum_{k_1,k_2} \phi_{k_1} \phi_{k_2} (-k_1^2) \langle \exp[ik_1 m(1) + ik_2 m(2)] \rangle \\ &= \sum_{k_1,k_2} \phi_{k_1} \phi_{k_2} (-k_1^2) \exp[-k_1^2 S_0(1)/2 - k_2^2 S_0(2)/2 \\ &\qquad\qquad -k_1 k_2 C_0(12)] \\ &= 2\, \partial C(12)/\partial S_0(1) . \end{aligned} \tag{88}$$

where $S_0(1)$, $S_0(2)$, are given by (77) and $C_0(12) = \langle m(1) m(2) \rangle$. The derivative in (88) is taken holding $S_0(2)$ and $C_0(12)$ fixed. Since, from the definition (75),

$\gamma(12) = C_0(12)/\sqrt{S_0(1)S_0(2)}$, the general result (79) for gaussian fields implies

$$2\frac{\partial C(12)}{\partial S_0(1)} = 2\frac{dC(12)}{d\gamma(12)}\frac{\partial \gamma(12)}{\partial S_0(1)}$$
$$= a(t)\,\gamma(12)\,\frac{dC(12)}{d\gamma(12)} \,. \qquad (89)$$

where

$$a(t) = 1/S_0(1) = \langle m(1)^2\rangle^{-1} \,. \qquad (90)$$

Putting it all together, and suppressing the arguments, the final equation for C is

$$(1/2)\,\partial_t C = \nabla^2 C + a(t)\,\gamma dC/d\gamma \,. \qquad (91)$$

Using (79) for $C(\gamma)$ gives $\gamma dC/d\gamma = (2/\pi)\tan[(\pi/2)C]$. Then (91) becomes a closed non-linear equation for C. For a scaling solution, one requires $L(t) \sim t^{1/2}$ and $a(t) = \lambda/2t$ for large t in (91), so that each of the terms scales as $1/t$ times a function of the scaling variable $r/t^{1/2}$. Setting $C(\mathbf{r},t) = f(r/t^{1/2})$ gives the equation

$$0 = f'' + \left(\frac{d-1}{x} + \frac{x}{4}\right) f' + \frac{\lambda}{\pi}\tan\left(\frac{\pi}{2}f\right) \qquad (92)$$

for the scaling function $f(x)$. The constant λ is fixed by the requirement that the large-distance behaviour of C be physically reasonable [50]. Linearization of (92) (valid for large x) leads to two linearly independent large-x solutions with gaussian and power-law tails. The constant λ is chosen to eliminate the 'unphysical' power-law term.

It is straightforward to adapt this approach to nonconserved vector fields [36, 37]. A significant simplification is that for gaussian fields, the joint probability distribution for $\vec{m}(1)$ and $\vec{m}(2)$ factors into a product of separate distributions of the form (76) for each component. This results is an equation of form (91) for any n, but with the function $C(\gamma)$ given by (84) for general n instead of (79). Again, $a(t) = \lambda/2t$, with λ chosen to eliminate the power-law tail in the scaling function $f(x)$. The values λ for various n and d are given in table 1.

It is interesting that the 'unphysical' power-law tails in real space become physical when sufficiently long-range spatial correlations are present in the initial state [44, 55].

The general two-time correlation function $C(\mathbf{r},t_1,t_2)$ can also be evaluated within this scheme [36, 37]. It is given by a simple generalization of (91), namely

$$\partial_{t_1} C = \nabla^2 C + a(t_1)\,\gamma dC/d\gamma \,, \qquad (93)$$

with $a(t_1) = \lambda/2t_1$. This equation simplifies for $t_1 \gg t_2$, because C is then small and the linear relation between C and γ for small C (see Eq. (84)) implies $\gamma dC/d\gamma = C$, i.e.

$$\partial_{t_1} C = \nabla^2 C + (\lambda/2t_1)\,C \,, \qquad t_1 \gg t_2 \,. \qquad (94)$$

This linear equation can be solved by spatial Fourier transform. Choosing an initial condition at $t_1 = \alpha t_2$, with $\alpha \gg 1$ to justify the use of (94) for all $t_1 \geq \alpha t_2$, gives

$$S(\mathrm{k},t_1,t_2) = \left(\frac{t_1}{\alpha t_2}\right)^{\lambda/2} \exp\{-k^2(t_1-\alpha t_2)\}\,S(\mathrm{k},\alpha t_2,t_2) \,. \qquad (95)$$

Imposing the scaling form $S(\mathrm{k},\alpha t_2,t_2) = t_2^{d/2} g(k^2 t_2)$, with $g(0) =$ constant, and Fourier transforming back to real space gives, for $t_1 \gg \alpha t_2$,

$$C(12) = \text{constant}\,\left(\frac{t_2}{t_1}\right)^{(d-\lambda)/2} \exp\left(-\frac{r^2}{4t_1}\right) \,. \qquad (96)$$

The constant cannot be determined from the linear equation alone: it is, of course, independent of α.

Comparison of (96) with the general form (60), shows that $\bar{\lambda} = d - \lambda$, i.e. the parameter λ of the Mazenko theory is precisely the exponent λ associated with the response function $G(\mathbf{k},t)$ (Eq. (66)), related to $\bar{\lambda}$ by (67). This connection was first pointed out by Liu and Mazenko [56]. The values of λ obtained (table 1) are in reasonable agreement with those extracted from simulations [15, 40, 58, 59]. For example, for the scalar theory in $d = 2$ simulations [15, 58, 56] give $\lambda \simeq 0.75$ (argued to be 3/4 exactly in [15]), compared to 0.711 from table 1.

d	n=1	n=2	n=3	n=4
1	0	0.301	0.378	0.414
2	0.711	0.829	0.883	0.912
3	1.327	1.382	1.413	1.432

Table 1 Exponent λ within the Mazenko theory.

To summarize, the virtues of Mazenko's approach are (i) only the assumption that the field m is gaussian is required, (ii) the scaling function has a non-trivial dependence on d (whereas, apart from the trivial dependence through the diffusion constant D, (75), (79) and (84) are independent of d), and (iii) the non-trivial behaviour of *different-time* correlation functions [16] emerges in a natural way [56]. In addition, the OJK result (79), and its generalization (84), are reproduced for $d \to \infty$, while the exact scaling function of the $1 - d$ Glauber model is recovered from (92) in the limit $d \to 1$ [60]. In practice, however, for $d \geq 2$ the shape of the scaling function $f(x)$ differs very little from that of the OJK function given by (79) and (75), or its generalization (84) for vector fields [37]. All these functions are in good agreement with numerical simulations. The Mazenko approach can also be used, with some modifications, for conserved scalar [51] and vector [57] fields.

To conclude this section we note that the crucial gaussian approximation, used in all of these theories, has recently been critically discussed by Yeung et al. [61]. By explicit simulation they find that the distribution $P(m)$ for the field m at a single point is flatter than a gaussian at small m. Recent work by Mazenko presents a first attempt to go beyond the gaussian approximation [62].

2.3.6 A Systematic Approach

All of the treatments discussed above suffer from the disadvantage that they invoke an uncontrolled approximation at some stage. Recently, however, a new approach has been developed [52] which recovers the OJK and BPT scaling functions in leading order, but has the advantage that it can, in principle, be systematically improved. For simplicity we will consider only scalar fields – the extension to vector fields is straightforward [52].

The TDGL equation for a non-conserved scalar field $\phi(\mathbf{x},t)$ is given by Eq. (2). We recall that, according to the Allen-Cahn equation (18), the interface motion is determined solely by the local curvature. It follows that the detailed form of the potential $V(\phi)$ is not important, a fact that we can usefully exploit: the principal role of the double-well potential is to establish and maintain well-defined interfaces.

Following Mazenko [50] we define the function $\phi(m)$ by Eq. (85) with boundary conditions $\phi(\pm\infty) = \pm 1$. We have noted that $\phi(m)$ is just the equilibrium domain-wall profile function, with m playing the role of the distance from the wall. Therefore, the spatial variation of m near a domain wall is completely smooth (in fact, linear).

The additional condition $\phi(0) = 0$ locates the center of the wall at $m = 0$. Figure 4 illustrates the difference between ϕ and m for a cut through the system. Note that, while ϕ saturates in the interior of domains, m is typically of order $L(t)$, the domain scale. Rewriting (2) in terms of m, and using (85) to eliminate V', gives

$$\partial_t m = \nabla^2 m - \frac{\phi''(m)}{\phi'(m)} (1 - (\nabla m)^2) \ . \tag{97}$$

For general potentials $V(\phi)$, Eq. (97) is a complicated non-linear equation, not obviously simpler than the original TDGL equation (2). For reasons discussed in section 2.1.3, however, we expect the scaling function $f(x)$ to be *independent* both of the detailed form of the potential and of the particular choice for the distribution of initial conditions. Physically, the motion of the interfaces is determined by their *curvature*. The potential $V(\phi)$ determines the domain wall *profile*, which is irrelevant to the large-scale structure.

Similarly, the initial conditions determine the early-time locations of the walls, which should again be irrelevant for late-stage scaling properties. For example, in Mazenko's approximate theory, both the potential and the initial conditions drop out from the equation for the scaling function $f(x)$.

The key step in the present approach is to exploit the notion that the scaling function should be independent of the potential (or, equivalently, independent of the wall profile) by choosing a particular $V(\phi)$ such that Eq. (97) takes a much simpler form (Eq. (101)). Specifically we choose the domain-wall profile function $\phi(m)$ to satisfy

$$\phi''(m) = -m\,\phi'(m) \ . \tag{98}$$

This is equivalent, via (85), to a particular choice of potential, as discussed below. First we observe that (98) can be integrated, with boundary conditions $\phi(\pm\infty) = \pm 1$ and $\phi(0) = 0$ to give the wall profile function

$$\phi(m) = (2/\pi)^{1/2} \int_0^m dx\, \exp(-x^2/2) = \mathrm{erf}\,(m/\sqrt{2}) \ , \tag{99}$$

where $\mathrm{erf}\,(x)$ is the error function. Also, (85) can be integrated once, with the zero of potential defined by $V(\pm 1) = 0$, to give

$$V(\phi) = (1/2)\,(\phi')^2 = (1/\pi)\,\exp(-m^2) = (1/\pi)\,\exp(-2[\mathrm{erf}^{-1}\,(\phi)]^2) \ , \tag{100}$$

where $\mathrm{erf}^{-1}\,(x)$ is the inverse function of $\mathrm{erf}\,(x)$. In particular, $V(\phi) \simeq 1/\pi - \phi^2/2$ for $\phi^2 \ll 1$, while $V(\phi) \simeq (1/4)(1-\phi^2)^2|\ln(1-\phi^2)|$ for $(1-\phi^2) \ll 1$.

With the choice (98), Eq. (99) reduces to the much simpler equation

$$\partial_t m = \nabla^2 m + (1 - (\nabla m)^2)\, m \ . \tag{101}$$

This equation, though still non-linear, represents a significant simplification of the original TDGL equation. It is clear, however, on the basis of the physical arguments discussed above, that it retains all the ingredients necessary to describe the universal scaling properties.

We now proceed to show that the usual OJK result is recovered by simply replacing $(\nabla m)^2$ by its average (over the ensemble of initial conditions) in (101), and choosing a gaussian distribution for the initial conditions. In order to make this replacement in a controlled way, however, and to facilitate the eventual computation of corrections to the leading order results, we systematize the treatment by attaching to the field m an internal 'colour' index α which runs from 1 to N, and generalize (101) to

$$\partial_t m_\alpha = \nabla^2 m_\alpha + (1 - N^{-1} \sum_{\beta=1}^{N} (\nabla m_\beta)^2)\, m_\alpha \ . \tag{102}$$

Eq. (101) is the case $N = 1$. The OJK result is obtained, however, by taking the limit $N \to \infty$, when $N^{-1} \sum_{\beta=1}^{N} (\nabla m_\beta)^2$ may be replaced by its average. In this limit (101) becomes (where m now stands for one of the m_α)

$$\partial_t m = \nabla^2 m + a(t)\, m \tag{103}$$

$$a(t) = 1 - \langle (\nabla m)^2 \rangle \,, \tag{104}$$

a self-consistent *linear* equation for $m(\mathbf{x}, t)$.

It is interesting that the replacement of $(\nabla m)^2$ by its average in (101) is also justified in the limit $d \to \infty$, because $(\nabla m)^2 = \sum_{i=1}^{d} (\partial m/\partial x_i)^2$. If m is a gaussian random field (and the self-consistency of this assumption follows from (103) – see below) then the different derivatives $\partial m/\partial x_i$ at a given point x are independent random variables, and the central limit theorem gives, for $d \to \infty$, $(\nabla m)^2 \to d\langle (\partial m/\partial x_i)^2 \rangle = \langle (\nabla m)^2 \rangle$, with fluctuations of relative order $1/\sqrt{d}$. While this approach is not so simple to systematize as that adopted above, it seems clear that the leading order results become exact for large d.

As discussed above, we will take the initial conditions for m to be gaussian, with mean zero and correlator (in Fourier space)

$$\langle m_{\mathbf{k}}(0)\, m_{-\mathbf{k}'}(0) \rangle = \Delta\, \delta_{\mathbf{k},\mathbf{k}'} \,, \tag{105}$$

representing short-range spatial correlations at $t = 0$. Then m is a gaussian field at all times. The solution of (103) is

$$m_{\mathbf{k}}(t) = m_{\mathbf{k}}(0) \exp(-k^2 t + b(t)) \,, \tag{106}$$

$$b(t) = \int_0^t dt'\, a(t') \,. \tag{107}$$

Inserting this into (104) yields

$$a(t) \equiv db/dt = 1 - \Delta \sum_{\mathbf{k}} k^2 \exp(-2k^2 t + 2b) \,. \tag{108}$$

After evaluating the sum one obtains, for large t (where the db/dt term can be neglected), $\exp(2b) \simeq (4t/\Delta d)\,(8\pi t)^{d/2}$, and hence $a(t) \simeq (d+2)/4t$. This form for $a(t)$ in (103), arising completely naturally in this scheme, reproduces exactly the Oono-Puri modification of the OJK theory [47], designed to keep the wall-width finite as $t \to \infty$, which was discussed in section 2.3.4.

The explicit result for $m_{\mathbf{k}}(t)$, valid for large t, is

$$m_{\mathbf{k}}(t) = m_{\mathbf{k}}(0)\, (4t/\Delta d)^{1/2}\, (8\pi t)^{d/4} \exp(-k^2 t) \,, \tag{109}$$

from which the equal-time two-point correlation functions in Fourier and real space follow immediately:

$$\langle m_{\mathbf{k}}(t)\, m_{-\mathbf{k}}(t) \rangle = (4t/d)\, (8\pi t)^{d/2} \exp(-2k^2 t) \,, \tag{110}$$

$$\langle m(1)\, m(2) \rangle = (4t/d) \exp(-r^2/8t) \,, \tag{111}$$

where '1', '2', are the usual shorthand for space-time points $(\mathbf{r}_1, t)$, $(\mathbf{r}_2, t)$, and $r = |\mathbf{r}_1 - \mathbf{r}_2|$.

We turn now to the evaluation of the correlation function of the original fields ϕ. Since, from (111), m is typically of order $\sqrt{t}$ at late times it follows from (99) that the field ϕ is saturated (i.e. $\phi = \pm 1$) almost everywhere at late times. As a consequence, the relation (99) between ϕ and m may, as usual, be simplified to $\phi = \mathrm{sgn}\,(m)$ as far as the late-time scaling behavior is concerned. Thus $C(12) = \langle \mathrm{sgn}\,(m(1))\, \mathrm{sgn}\,(m(2)) \rangle$. The calculation of this average for a gaussian field m proceeds just as in the OJK calculation. The OJK result, given by (79) and (75), (with $D = 1$) is recovered. The present approach makes possible, in principle, a systematic treatment in powers of $1/N$, although technical difficulties have thus far prevented this programme being put into practice.

2.4 Aging

Consider the following experiment. The system is quenched into the ordered phase at time $t = 0$, and left to evolve for a time t_w. Then a perturbation is applied (e.g. a magnetic field is switched on), and the response to the perturbation (the magnetization) is monitored. Since the system is in a nonequilibrium state at time t_w, it is to be expected that the subsequent response will depend explicitly on the waiting time t_w. This effect is termed 'aging', and plays an important role is the study of spin-glass systems where nonequilibrium dynamics is endemic. The same type of phenomenon, however, can be observed also in simple coarsening systems of the type we have been discussing.

An explicit, albeit approximate, calculation is possible using an approach of the OJK type. (The 'systematic approach' of section 2.3.6 is cleaner, but more complicated [1]). Let up apply a magnetic field after time t_w. In terms of the approach adopted in section 2.1.3, an external field corresponds to having a potential with minima of unequal depths. Then the interface equation (18) is modified to $v = -K + \Delta V/\sigma$, where ΔV is the potential difference between the minima, and σ the surface tension. If the minimum corresponding to $\phi > 0$ is the lower, then $\Delta V < 0$ and I will introduce $h = -\Delta V/\sigma$ as a 'magnetic field'. The interface equation then becomes $v = -K - h$. Following the same steps as in section 2.3.3, the equation for the auxiliary field m reads

$$\partial m/\partial t = \nabla^2 m - n_a n_b \nabla_a \nabla_b m + h|\nabla m|. \tag{112}$$

In addition to the approximation $n_a n_b \to \delta_{ab}/d$ made before, we need a further approximation to simplify the final term. The simplest is the replacement $|\nabla m| \to \langle(\nabla m)^2\rangle^{1/2}$. With these approximations, (112) becomes

$$\partial m/\partial t = D\nabla^2 m + a(t)h, \tag{113}$$

where $D = (d-1)/d$ and $a(t) = \langle(\nabla m)^2\rangle^{1/2}$.

Eq. (113) is now linear, and can be solved. The Fourier components $\mathrm{k} \neq 0$ are unaffected by the field so, since $a(t)$ involves only these components, one has $a(t) = [\sum_{\mathbf{k}} k^2 \langle m_{\mathbf{k}}(t) m_{-\mathbf{k}}(t)\rangle]^{1/2} \sim \sqrt{\Delta}/t^{(d+2)/4}$ up to constants. The mean value of $m(t)$ (for $t > t_w$) is given by $\langle m(t)\rangle \sim \sqrt{\Delta}\int_{t_w}^{t} dt'\, h(t')/t'^{(d+2)/4}$, allowing for a time-dependent field. The variance of m is the second cumulant $\langle m^2\rangle_c \sim \Delta/t^{d/2}$. Finally, the expectation value of the order parameter ϕ is $\langle\phi\rangle = \mathrm{erf}(\langle m\rangle/\sqrt{2\langle m^2\rangle_c})$, which follows from the gaussian property of m. Expanding out the argument of the error function for small fields gives

$$\langle\phi(t)\rangle \sim t^{d/4}\int_{t_w}^{t} dt' h(t')/t'^{(d+2)/4}. \tag{114}$$

Let us define the response function $G(t,t') = \delta\langle\phi(t)\rangle/\delta h(t')$. Then $G(t,t')$ can be written in the form

$$G(t,t') = t'^{-1/2}\,[L(t)/L(t')]^{d/2}. \tag{115}$$

For a constant field, (114) gives, for $t \gg t_w$, $m(t) \sim ht^{1/2}$ for $d < 2$, and $m(t) \sim ht_w^{1/2}(t/t_w)^{d/4}$ for $d > 2$, the latter case retaining an explicit dependence on t_w even for $t \gg t_w$.

This result is a special case of a more general result that can be deduced using scaling arguments [63]. The response function $G(t,t')$ is the magnetization at time t due to a field pulse at time t'. The effect of the pulse is to induce a small bias (i.e. a non-zero magnetization) which then grows spontaneously under the subsequent dynamics. Consider first the effect of a small bias in the initial condition. The exact result (66), with $\mathrm{k} = 0$ for a uniform bias, shows that an initially small magnetization grows with time as $L(t)^{\lambda}$. Now suppose that the bias is introduced, not in the initial

condition, but at time t' when the system is already in the scaling state. Then scaling implies $m(t) = m(t')f[L(t)/L(t')]$ for $t > t'$, where $f(x)$ is a scaling function with the properties $f(1) = 1$ and $f(x) \sim x^\lambda$ for large x. To determine $m(t')$, we note that a magnetic field h induces a systematic term in the velocity v of the domain walls. The 'net' volume (in the sense of increasing magnetization) swept out by the walls in a time interval Δt is proportional to $h\Delta t$ and to the total interfacial area, which scales as $1/L(t')$. The induced magnetization is therefore $m(t') \sim h\Delta t/L(t')$, giving $G(t,t') = [1/L(t')]f[L(t)/L(t')]$. Recalling that $L(t) \sim t^{1/2}$, we see that this result has the same form as (115), where $f(x) = x^{d/2}$ (recall that $\lambda = d/2$ in the OJK theory). Inserting the general form for G into $m(t) = \int_{t_w}^{t} dt'\, G(t,t')h(t')$, and taking a constant field, gives, for $t \gg t_w$, $m(t) \sim ht^{1/2}$ for $\lambda < 1$ and $m(t) \sim ht_w^{1/2}(t/t_w)^{\lambda/2}$ for $\lambda > 1$. Hence $\lambda = 1$ replaces $d = 2$ as the boundary between the two regimes. In practice, $\lambda > 1$ for $d \geq 3$ (see, e.g., table 1).

3 Coarsening in Disordered Systems

3.1 Disordered Ferromagnets

The influence of quenched disorder on the motion of interfaces and other defects is of considerable current interest in a variety of contexts. The new ingredient when quenched disorder is present is that the defects can become pinned in energetically favourable configurations. At $T = 0$ this leads to a complete cessation of growth. For $T > 0$, thermal fluctuations can release the pins, but in general growth is much slower than in 'pure' systems - typically logarithmic in time.

To see how logarithms arise, consider a single domain wall in a system with quenched random bonds. The typical transverse displacement of the wall over a length l, due to disorder roughening, is of order l^ζ, while the typical fluctuation of the wall energy around its mean value is of order l^χ. These exponents are related by the scaling law [64] $\chi = 2\zeta + d - 3$, which can be obtained by estimating the elastic energy of the deformed wall as $l^{d-1}(l^\zeta/l)^2$, and noting that the pinning and elastic energies should be comparable. The barrier to domain motion can be estimated by arguing [64, 65, 66, 67] that the walls move in sections of length l, where l is the length scale at which the walls 'notice' their curvature, i.e. the disorder roughening l^ζ should be comparable to the distortion, of order $l^2/L(t)$, due to the curvature of walls with typical radius of curvature $L(t)$. This gives $l \sim L^{1/(2-\zeta)}$ and an activation barrier of order $l^\chi \sim L^{\chi/(2-\zeta)}$ (assuming that the energy *barriers* scale in the same way as the energy *fluctuations* between local equilibrium positions of the wall). Equating this barrier to T gives a growth law

$$L(t) \sim (T \ln t)^{(2-\zeta)/\chi} . \tag{116}$$

For $d = 2$, the exponents ζ and χ are exactly known [68]: $\zeta = 2/3$ and $\chi = 1/3$, giving $L(t) \sim (T \ln t)^4$. A number of attempts to measure $L(t)$ in computer simulations have been made [69, 70, 71], but it is difficult to obtain a large enough range of $(\ln t)^4$ for a convincing test of the theoretical prediction. Recent experimental studies of the two-dimensional random-exchange Ising ferromagnet $Rb_2Cu_{0.89}Co_{0.11}F_4$, however, suggest $L(t) \sim (\ln t)^{1/\psi}$ with $\psi = 0.20 \pm 0.05$ [72], consistent with the theoretical prediction $\psi = 1/4$.

Perhaps of greater interest than the growth law itself is the universality class for the *scaling functions*. It can be argued [15] that, since $L \gg l \sim L^{1/(2-\zeta)}$ for $L \to \infty$ (note that $\zeta < 1$ for a system above its lower critical dimension, otherwise disorder-induced roughening would destroy the long-range order), on length scales of order L the driving force for domain growth is still the interface curvature: the pinning at smaller scales serves merely to provide the (scale-dependent) renormalization of the kinetic coefficient responsible for the logarithmic growth. This leads to the

conclusion [15] that the scaling functions should be identical to those of the pure system, a prediction that is supported by numerical studies [70, 71]. The same prediction can be made for systems with random-field (i.e. local symmetry-breaking) disorder [15], and is supported by recent simulations [73]. A further consequence of this idea is that the autocorrelation exponent $\bar{\lambda}$, defined through $[\langle S_i(t)\langle S_i(0)\rangle]_{av} \sim L(t)^{-}\bar{\lambda}$, should also be the same for pure and disordered ferromagnets, and there is support for this idea from numerical simulations [70].

It is interesting that the argument leading to (116) makes no reference to whether the order parameter is conserved or not. The time taken to surmount the pinning barriers dominates all other timescales in the problem. The argument outlined above suggests a scale-dependent kinetic coefficient $\Gamma(L) \sim \exp(-L^{\chi/(2-\eta)}/T)$. Putting this into the usual nonconserved growth law $L \sim [\Gamma(L)t]^{1/2}$ gives $L \sim [T\ln(t/L^2)]^{\chi/(2-\zeta)}$, which reduces to (116) asymptotically, since $\ln L \ll \ln t$ for $t \to \infty$. For conserved dynamics, the same argument just gives t/L^3 instead of t/L^2 inside the logarithm, and (116) is again recovered asymptotically.

While this physically based argument is certainly plausible, the RG approach developed in [1] makes a more powerful prediction: not only are the growth laws the same for conserved and nonconserved dynamics, but they belong to the *same universality class*! This means, *inter alia*, that they have the *same scaling functions*! To see this, we simply note that since the *fluctuations* in the interfacial free energy, $\delta F \sim L^{\chi}$, are asymptotically negligible compared to the *mean*, $\langle F\rangle \sim L^{d-1}$ (provided the system supports an ordered phase at infinitesimal T), the strong-coupling exponent y (defined by $F \sim L^{y}$: see section III for a more detailed discussion of y) is given by the same expression, $y = d-1$, as in the pure system. (Alternatively, and equivalently, the extra area of domain wall due to disorder roughening of the interfaces in a volume L^d scales as $\sim L^{d-3+2\zeta} \ll L^{d-1}$). In [1, 74] it was shown that, *provided the conservation law is relevant*, the dynamical exponent z (defined by $L(t) \sim t^{1/z}$) for conserved systems is generally related to y through $z = d+2-y$, which gives the usual $t^{1/3}$ growth for pure systems (using $y = d-1$). However, one can also show [74] that if this result predicts a *faster* growth than that of the corresponding *nonconserved* system, the conservation law must be irrelevant, and the nonconserved scaling results are recovered – physically this is the statement that the conservation can only slow down the dynamics, not speed it up. Since the growth for disordered systems is logarithmic in time, i.e. slower than the $t^{1/3}$ growth predicted assuming the conservation law is relevant, it follows that the conservation law is *irrelevant* for systems with quenched disorder. Therefore conserved and nonconserved systems are in the same universality class.

Numerical simulations [75, 76] allow us in principal to test this prediction. They certainly show logarithmic growth, but with an insufficient range of L for a definitive test of (116). The most striking conclusion of the RG is that the scaling functions are those of the nonconserved system. For example, a scaling plot for the structure factor, i.e. a plot of $L^d S(k,t)$ against kL should give a non-zero intercept at $kL = 0$. For any fixed L, of course, the conservation law requires that S vanish at $k = 0$, but in the scaling limit ($k \to 0$, $L \to \infty$, with kL fixed) the region of small k where the conservation law is effective should shrink to zero faster than $1/L$ as $L \to \infty$. There are indeed indications of this in the small-k data of Iwai and Hayakawa [76], but the range of L explored in not large enough to reach the true scaling limit. Indeed, this will always be difficult with growth as slow as (116).

3.2 Spin Glasses within the Droplet Theory

The 'droplet' or scaling theory emerged around ten years ago as a coherent, albeit phenomenological, theory of the ordered phase due to the work of a number of authors [77, 78, 79, 80, 81, 82, 83, 80, 84, 15]. It is based on an alternative scenario to the mean-field SK model for the description of finite-dimensional spin glasses. The fundamental concept is a 'generalized stiffness constant', Υ, analogous to to the surface tension of an Ising ferromagnet, or the spin-wave stiffness of a Heisenberg

ferromagnet: Υ measures the sensitivity of the free energy to changes in the boundary conditions and provides a useful 'macroscopic order parameter' which requires no knowledge of the underlying spin order.

In an Ising ferromagnet, the free energy of an interface between domains of opposite magnetization scales with the linear dimension L as L^{d-1}. The (temperature-dependent) coefficient of L^{d-1} is the surface tension $\sigma(T)$. By contrast, for a spin glass the interfacial free energy scales as L^y, with $y < d-1$ as a consequence of frustration. The exponent y is the fundamental exponent characterizing the spin-glass phase: all quantities which are dominated by large scale excitations ('droplets') are described by power-laws with exponents related to y, and the sign of y determines whether the system orders at $T > 0$ ($y > 0$) or not ($y < 0$). It has not proved possible to determine y analytically except for $d = 1$ [78, 80]. Note that y is not a *critical* exponent, but an exponent associated with the ordered phase, in particular the $T = 0$, or 'strong-coupling', RG fixed point. The associated phenomenology is, therefore, sometimes referred to as 'zero-temperature scaling'.

3.2.1 Zero-Temperature Scaling

It is instructive to first the simple Ising ferromagnet. Consider a hypercube of linear dimension L. For periodic boundary conditions, the ground state has all spins parallel. Now impose *antiperiodic* boundary conditions in one direction. The ground state now has a domain wall separating regions of up and down spins, a shown in Figure 5(a). Each 'broken bond' cost energy $2J$ relative to the ground state energy, so the energy of the domain wall is $2JL^{d-1}$, i.e. the exponent y is $d-1$. For $y > 0$, i.e. $d > 1$, the energy required to create large droplets of overturned spins increases with the size L of the droplets as L^{d-1}. At low temperatures this energy is not available as thermal energy, and the ordered phase is stable against the spontaneous creation of large droplets by thermal fluctuations for $d > 1$. The 'lower critical dimension of the Ising ferromagnet is $d_l = 1$.

Similar ideas can be applied to Heisenberg (or planar) ferromagnets. Now antiperiodic boundary conditions in one direction induce a smooth twist in the spin configuration instead of a sharp discontinuity (Figure 5(b)). Since the angle between neighbouring spins is of order $1/L$, the energy cost per horizontal bond scales as L^{-2}, and the total energy cost associated with the antiperiodic boundary conditions scales as L^{d-2}. The exponent y is $d-2$, and the lower critical dimension is $d_l = 2$.

In applying the same idea to spin glasses we note that it is not possible to compute the ground-state energy analytically for either boundary condition (periodic or antiperiodic), and that the two boundary conditions have equal *a priori* probability to give the lower energy (for the case where the distribution $P(J)$ of exchange interactions is symmetric), i.e. the domain wall energy will be symmetrically distributed around zero. Therefore one has to consider a large number of samples to construct the probability distribution of domain wall energies. If E is the energy of a wall, $P_L(E)$ is the distribution of E for samples of size L. We consider only the case of *symmetric* [i.e. $P(J) = P(-J)$], *continuous* (e.g. gaussian) distributions of exchange couplings. Numerical studies of small systems suggest that $P_L(E)$ approaches, for large L, the scaling form $P_L(E) = (1/E_s)f(E/E_s)$, with scale energy $E_s \sim JL^y$, where J is a typical (e.g. rms), exchange interaction. The energy E_s could, for example, be the rms wall energy $E_s = \langle E^2 \rangle^{1/2}$. These numerical studies give $y < 0$ for $d = 2$ ($y \approx -0.3$), while $y > 0$ for $d = 3$ ($y \approx 0.2$). Thus the lower critical dimension lies between 2 and 3. These studies also show that the scaling function $f(x)$ has weight at the origin, $0 < f(x) < \infty$. This implies that, even for $d = 3$, large domains *can* be thermally excited at a small temperature T, since there is a small probability, of order T/JL^y, the domain wall energy is smaller than T.

For $d = 2$ there is a phase transition at $T = 0$ and, within the droplet theory, the exponent y determines the 'critical exponents' for this transition. We have argued that, since $y < 0$ for $d = 2$, there can be no ordered phase for any $T > 0$ since arbitrarily large domains will be thermally excited. There will, however, be

short-range order since domains (or 'droplets') of size L such that $JL^y > T$ will *not* be thermally excited, i.e. the system will be ordered on length scales shorter than $\xi \sim (J/T)^{1/|y|}$. Hence ξ is the correlation length for this 'zero-temperature transition', and diverges for $T \to 0$ as $T^{-\nu}$, with $\nu = 1/|y|$.

The above arguments can be rephrased can be rephrased in RG language. The typical domain-wall energy becomes a scale-dependent, or 'running', coupling constant, i.e. $P_L(J)$ becomes the distribution of effective couplings for a system which has been coarse-grained at scale L. The scale-width of the distribution, $J_s \sim JL^y$, scales to infinity ('strong coupling') with increasing L if $y > 0$, and to zero ('weak coupling') if $y < 0$. Thus, at infinitesimal T, the system looks 'more ordered' at large length scales if $y > 0$, and 'more disordered' if $y < 0$. Since physical properties only depend on the dimensionless ratios $\{J_{ij}/T\}$, we can reinterpret the flow of the characteristic coupling under coarse graining as a flow of temperature: an initially small T decreases (increases) with increasing length scale for $y > 0$ ($y < 0$). The $T = 0$ fixed point is stable (unstable) for $y > 0$ ($y < 0$). Schematic RG flows are shown in Figure 6.

The concept of a domain-wall energy can be be generalized to $T > 0$ as a domain-wall *free* energy. Since, for all $T < T_c$, the system flows to $T = 0$ under coarse-graining, the distribution of domain-wall free energies should approach, for large L, the same fixed shape as at $T = 0$. The scale width F_s (e.g. the rms value) varies as L^y, but with a T-dependent prefactor: $F_s = \Upsilon(T)L^y$. The generalized stiffness $\Upsilon(T)$ has its maximum value at $T = 0$ and vanishes at $T = T_c$.

3.2.2 Statics

Here we use the ideas developed above to obtain a qualitative description of the ordered phase of an Ising spin glass within the droplet model. We first discuss the spin correlations in the ordered phase, and then address the role of an external magnetic field.

For a particular sample one can define the 'connected' correlation functions

$$C_{ij} = \langle S_i S_j \rangle_T - \langle S_i \rangle_T \langle S_j \rangle_T, \tag{117}$$

where $\langle ... \rangle_T$ indicates a thermal average. Since C_{ij} varies randomly from sample to sample, and from one spin pair (i, j) to another, it is convenient to compute instead an average over samples. The first moment, $[C_{ij}]_{av}$, vanishes by symmetry for a bond distribution symmetric about $J = 0$. Therefore, one usually considers the second moment

$$G(r_{ij}) = [C_{ij}^2]_{av}. \tag{118}$$

Consider first a system at infinitesimal temperature. The correlation C_{ij} is zero for most pairs (i, j), since the pairs are locked into the ground-state configuration and the second term in (117) cancels the first. Non-zero contributions to $G(r)$ come from those pairs (i, j) which can be enclosed by a domain wall whose energy E is small compared to T. For such a pair $|C_{ij}| = 1$, since $S_i S_j$ is invariant under a reversal of the domain while S_i and S_j separately change sign. For $E \ll T$, the domain (or droplet) is completely thermalized, i.e. equally likely to be in either of its two configurations, giving $\langle S_i \rangle_T = 0 = \langle S_j \rangle_T$, while $|\langle S_i S_j \rangle_T| = 1$. The probability that the pair (i, j) belong to such a thermalized droplet is of order T/Jr^y (where Jr^y is an estimate of the excitation energy of the droplet, and r is the separation of the spins). Since $|C_{ij}|$ is of order unity for such pairs, and zero otherwise, these arguments give [83]

$$G(r) \sim T/Jr^y, \quad T \ll T_c. \tag{119}$$

This result may equivalently be derived [80] using the RG ideas outlined above. After coarse-graining at a scale comparable to the spin separation r, the distribution of effective exchange interactions has a width of order Jr^y. At the same time, the spins S_i and S_j become members of the same 'block spin' σ, giving $G(r) = 1 - [\langle \sigma \rangle_T^2]_{av}$. Non-zero contributions to $G(r)$ come from block spins which are thermally

decoupled from their neighbours, in the sense that the net field due to the neighbours is small compared to T. A fraction of order T/Jr^y of the block spins satisfies this condition, giving $G(r) \sim T/Jr^y$ as before. Note that fluctuations on length scales smaller than r have not been considered in this argument. These play a role when general temperatures $T < T_c$ are considered. They lead to a reduction factor $\sqrt{q}$ in the effective size of the block spin, where $q = [\langle S_i \rangle_T^2]_{av}$ is the Edwards-Anderson order parameter. In addition, the scale width of the distribution of effective couplings contains, at general T, the factor $\Upsilon(T)$. Putting these factors together yields [80, 83]

$$G(r) \sim Tq^2/\Upsilon r^y, \quad T < T_c. \tag{120}$$

To discuss the effect of an applied magnetic field, we use simple ideas based on droplet energetics, along the lines of the Imry-Ma argument for random magnetic fields in ferromagnets [86]. The alternative approach based on RG ideas gives the same results.

Consider first $T = 0$. The idea is that in the presence of the field, it may be energetically favourable for the zero-field ground state to break up into large domains that independently align with the field [79, 83]. This will happen if the energy cost of the domain walls formed is smaller than the Zeeman energy gained by aligning the domains with the field. Suppose the domains have typical linear dimension L. Then the wall energy of a domain is of order $E_{wall} \sim JL^y$. Since the spins in the unperturbed ground state are randomly oriented with respect to the external field h, the magnetization M of a domain is of order $L^{d/2}$, leading to a Zeeman energy of order $E_{Zeeman} \sim -hL^{d/2}$. Provided $y < d/2$, the volume term will dominate at sufficiently large L, and the zero-field ground state will be unstable against large-scale reorientation of domains. Since the number of domains per site is of order L^{-d}, the change in the energy per spin due to domain formation is of order $\delta E \sim JL^{y-d} - hL^{-d/2}$. Minimizing with respect to L yields

$$L \sim (J/h)^{2/(d-2y)}. \tag{121}$$

These arguments can be used to compute the macroscopic magnetization induced by the field. Each domain has a magnetization of order $L^{d/2}$, and hence a magnetization per site of order

$$m \sim L^{-d/2} \sim (h/J)^{d/(d-2y)}. \tag{122}$$

Since the domains independently align with the field, this is also the macroscopic magnetization per site. Eq. (122) shows that the magnetization is *non-analytic* in the field in the ordered phase [79]. Actually, (122) gives the *singular* part of the response. There is also a regular contribution of the form $m_{reg} = \chi h$ due to isolated spins and finite clusters overturning in the field, i.e. to small-scale reorientations induced by the field. By contrast, the singular contribution is due to large-scale reorientations (note that $L \to \infty$ as $h \to 0$). The generalization to $T > 0$ is accomplished through the replacements $J \to \Upsilon$, $h \to h\sqrt{q}$, accounting for the reduction in the interfacial stiffness and the domain magnetization respectively due to thermal fluctuations [80].

An important consequence of these arguments is that, within the droplet model, a magnetic field removes the spin-glass phase transition. In RG terminology, the magnetic field is a 'relevant perturbation' for $d/2 > y$. Since the domains align independently with the field, there are no long-range spin correlations for non-zero field. Indeed, the equilibrium domain size L can be interpreted as a field-dependent correlation length $\xi(h)$. The 'Almeida-Thouless line', which in SK model marks the onset of spin-glass order in a field [85], is absent from the 'droplet model'. There should, however, be a 'dynamic AT line', observable in experiments with fixed timescales or frequencies.

3.2.3 Dynamics

Assuming that the dynamics of the ordered phase is described by activation over barriers, Fisher and Huse [83] introduced a scale-dependent barrier height $B(L) \sim bL^{\psi}$.

The corresponding scale-dependent relaxation time is given by the Arrhenius form $\ln[\tau(L)/\tau_0] \sim (b/T)L^\psi$, with τ_0 a microscopic timescale. In a magnetic field h, there is a maximum relaxation time, associated with length scales of the order of the correlation length $\xi(h)$. Using (121) for $\xi(h)$ yields $\ln(\tau_{max}/\tau_0) \sim (b/T)(J/h)h^{2\psi/(d-2y)}$. This result is for infinitesimal T. The temperature-dependence can be inserted through the replacements $J \to \Upsilon(T)$, $h \to \sqrt{q}h$ as before, and $b \to b(T)$. For $T \to T_c$ one can express $q(T)$, $\Upsilon(T)$ and $b(T)$ in terms of conventional critical exponents: $q \propto (T_c - T)^\beta$, $\Upsilon \propto (T_c - T)^{y\nu}$, and $b \propto (T_c - T)^{\psi\nu}$, where the last two follow from the assumption that interfacial energies and free-energy barriers are scale invariant at T_c. With these replacements, one obtains

$$h^2/T_c^2 \sim [\ln(\tau_{exp}/\tau_0)]^{-(d-2y)/\psi}(1 - T/T_c)^\phi \tag{123}$$

for the dynamic AT line on experimental time scale τ_{exp}. Here $\phi = \beta + \gamma$ is the usual crossover exponent associated with h^2, and the scaling law $d\nu = 2\beta + \gamma$ has been used. Eq. (123) has the form predicted by conventional critical scaling, but with a prefactor that depends on the experimental time scale. Thus the dependence of the position of an apparent AT line on experimental time scale or frequency determines the exponent combination $(d-2y)/\psi$ within the droplet model. Indeed, the existence or nonexistence of an equilibrium AT line is a key discriminant between the rival theories of the spin-glass ordered phase.

Similar arguments involving relaxation over barriers have been used to determine the behaviour of temporal correlation functions in equilibrium [83]. For example, the equilibrium spin-spin autocorrelation function

$$C(t - t') = [\langle S_i(t)S_i(t')\rangle_T - \langle S_i(t)\rangle_T\langle S_i(t')\rangle_T]_{av} \tag{124}$$

is dominated by excitations which just fail to relax on time scale t. Such excitations have length scale $L(t) \sim \{(T/b)\ln(t/\tau_0)\}^{1/\psi}$, and the probability that such an excitation is thermalized (so that $\langle S_i(t)\rangle_T = 0$) is of order $T/\Upsilon L(t)^y$, giving

$$C(t) \sim (Tq/\Upsilon)\{(T/b)\ln(t/\tau_0)\}^{-y/\psi}, \tag{125}$$

a logarithmically slow decay which leads to $1/f$ noise (up to logarithmic corrections) in the power spectrum of the equilibrium magnetization fluctuations [83]. However, the dynamics is so slow in the ordered phase that equilibrium correlations are in practice unobservable. Instead, one must consider nonequilibrium correlations.

3.2.4 Coarsening

From the scale-dependence of the (free-)energy barriers, $B(L) \sim bL^\psi$, it follows that the coarsening length scale in a spin glass grows as $L(t) \sim (\ln t)^{1/\psi}$. The 'domains' consist of the two 'pure phases' (one being the global inverse of the other) of the droplet model. In contrast to ferromagnetic systems, however, the domain walls are believed to be fractal, i.e. the interfacial length of a section of wall of linear dimension L scales as L^{d_s}, with $d - 1 < d_s < d$. Measurements of d_s through numerical studies give $d_s \approx 1.26$ for $d = 2$ [87], and ≈ 2.2 for $d = 3$ [88]. It follows that the domain-wall density scales as

$$\rho(t) \sim L(t)^{d_s - d} \tag{126}$$

for spin glasses, instead of $L(t)^{-1}$.

Huse [88] has measured $\rho(t)$ by looking at the overlap between two replicas (i.e. systems with identical bonds) coarsening from independent random initial conditions. He defines the local overlap $\Omega_i(t) = \sigma_i^1(t)\sigma_i^2(t)$, where the superscripts are replica indices and $\sigma_i^\alpha(t) \equiv \mathrm{sgn}[\sum_{\tau=t/2}^t S_i^\alpha(\tau)]$ is a time-averaged local magnetization intended to average over short-term thermal fluctuations. If one defines 'domains'

for Ω as regions where Ω_i has a given sign, then these domains should coarsen in much the same way as the 'real' domains of the underlying replicas, since Ω has a domain walls wherever either (but not both) of the replicas has a wall. The average domain size $L(t)$ was found from looking at the distance from each site to the nearest wall along the lattice axes, and averaging over axes and sites. Monte Carlo simulations in $d = 3$ gave a result consistent with (126), with $d - d_s \approx 0.83$, i.e. $d_s \approx 2.17$. The dependence of $L(t)$ on $\ln t$ suggested an exponent ψ a little less than unity.

The reasonable fit to a power-law decay of $\rho(t)$, suggesting that $\rho(t)$ vanishes for $t \to \infty$, is consistent with the droplet theory: at $t = \infty$, both replicas would either be in the same phase or different phases, so Ω_i would be 1 or -1 everywhere, with no domain walls. In the alternative scenario, based on Parisi's solution of the SK model, there are many pure phases. If the two replicas settle into different phases (unrelated by symmetry), the overlap function Ω_i would exhibit domain walls (where the two phases differ) even in equilibrium, and $\rho(t)$ would saturate at some non-zero limiting value. Since $\rho(t)$ only decays by a factor of two in the simulations, however, the present data should not be seen as conclusive. It may be worth repeating these simulations, using Derrida's method [89] of eliminating the effects of thermal fluctuations, rather than the crude time-averaging adopted by Huse.

Finally we note that aging phenomena in spin glasses can also be discussed within the droplet model. Since this goes beyond the scope of the present lectures, I refer the interested reader to the paper by Fisher and Huse [15].

4 Persistence in Coarsening Processes

4.1 What is Persistence?

In addition to the exponents z and $\bar{\lambda}$ which describe the growth of the domain scale ($L(t) \sim t^{1/z}$) and the decay of autocorrelations ($A(t) \sim L(t)^{-\bar{\lambda}}$) respectively, there has been recent interest in a new exponent θ which describes the 'persistence' of local degrees of freedom (e.g. spins) in the coarsening state. The 'persistence' probability, $p(t_1, t_2)$, is the probability that the order parameter $\phi(\mathbf{x}, t)$, or the spin $S_i(t)$, for a particular point $\mathbf{x}$ or site i, has not changed sign between times t_1 and t_2 (where t_1 is often taken to be the quench time, $t_1 = 0$). For coarsening at $T = 0$, one expects that this probability will have the scaling form $p(t_1, t_2) = f(t_2/t_1)$ when both times correspond to the asymptotic scaling state. The function $f(x)$ is generically found to have a power-law tail, $f(x) \sim x^{-\theta}$, for $x \to \infty$, i.e. $p(t_1, t_2)$ decays as $t_2^{-\theta}$ for fixed t_1. The exponent θ has been called the 'persistence exponent'.

The power-law tail is restricted to coarsening at $T = 0$, since thermal activation at $T > 0$ will lead to an exponential decay of the persistence probability. For $T > 0$, one needs to define persistence in a generalized way as the probability that a particular point in space has remained in the same *phase* for $t_1 < t < t_2$. A method of measuring, in numerical simulations, persistence defined this way has recently been proposed by Derrida [89]. In the present notes, we will restrict discussion to coarsening at $T = 0$ and, for simplicity, we will model the coarsening through the approximate OJK theory for a nonconserved scalar field discussed in section 2.3.3. Recall that the auxiliary field m is gaussian within this approximation, and obeys the simple diffusion equation. Since m and the order parameter ϕ have the same zeros, we can conveniently discuss persistence in terms of the field m. Given the ubiquity of the diffusion equation in physics, the results will be of interest beyond the field of phase-ordering kinetics considered here. In the following, we use the symbol ϕ to represent the diffusion field. It should be borne in mind that, in the phase-ordering context, ϕ now represents the gaussian field m, not the order parameter field. The results presented below were derived independently by two groups [90, 91].

4.2 Persistence in the Diffusion Equation

The diffusion equation, $\partial_t \phi = \nabla^2 \phi$, is one of the fundamental equations of classical physics. The exact solution of this simple equation, for an arbitrary initial condition $\phi(\mathbf{x}, 0)$, can be written down explicitly: $\phi(\mathbf{x}, t) = \int d^d x\, G(\mathbf{x} - \mathbf{x}', t)\phi(\mathbf{x}', 0)$, where $G(\mathbf{x}, t) = (4\pi t)^{-d/2} \exp(-x^2/4t)$ is the Green's function (or 'heat kernel') in d dimensions. The solution is characterized by a single growing length scale, the 'diffusion length' $L(t) \sim t^{1/2}$. It is somewhat surprising, therefore, to discover that there is a nontrivial exponent associated with this simple process.

In the following we point out that the solutions of the diffusion equation exhibit some unexpected properties associated with their time evolution, and to present a simple theory which accounts for this behavior. We consider specifically a class of initial conditions where $\phi(\mathbf{x}, 0)$ is a gaussian random variable with zero mean. Our basic question is the following. What is the probability $p_0(t)$ that the field ϕ at a particular point $\mathbf{x}$ has not changed sign up to time t? Precise numerical simulations in $d = 1$ and 2, discussed below, demonstrate a power-law decay of the form $p_0(t) \sim t^{-\theta}$, with $\theta = 0.1207 \pm 0.0005$ for $d = 1$, and 0.1875 ± 0.0010 for $d = 2$. We will present a simple analytic treatment which gives results in extraordinarily good agreement with the simulations. Furthermore, the analysis gives the more general result $p_n(t_1, t_2) \sim [\ln(t_2/t_1)]^n (t_1/t_2)^{-\theta}$ for the probability that the field changes sign n times between t_1 and t_2, for $t_2 \gg t_1$. The key idea underlying these results is that the gaussian process $\phi(\mathbf{x}, t)$ is a gaussian *stationary* process in terms of a new time variable $T = \ln t$. The central assumption in the analysis is that the intervals between successive zeros of $\phi(\mathbf{x}, T)$ can be treated as independent.

Exponents θ analogous to that introduced above have recently excited much interest in a variety of contexts [92, 93, 94, 95, 96, 97, 98, 99, 100, 101, 102, 103]. The simplest such system is the $d = 1$ Ising model at temperature $T = 0$. For evolution under Glauber dynamics from a random initial state , the probability that a given spin has not flipped up to time t decays as $t^{-\theta}$, with $\theta = 3/8$, though the proof of this is surprisingly subtle [97]. This $d = 1$ method is difficult to extend to higher dimensions, although values for θ have been obtained numerically [92, 94, 95, 98]. An approximate method for general dimensions has recently been developed [98], whose predictions are consistent with simulation results. In general, the non-triviality of $p_0(t)$ is a consequence of the fact that it probes the entire history of a *non-Markovian* process.

We begin by presenting the theoretical approach and the numerical simulation results. Experimental ramifications will be discussed briefly. Other contexts in which a nontrivial exponent θ might be expected will also be discussed.

The starting point for the discussion of the diffusion equation is the expression for the autocorrelation function of the variable $X(t) = \phi(\mathbf{x}, t)/\langle[\phi(\mathbf{x}, t)]^2\rangle^{1/2}$ for some fixed point $\mathbf{x}$. For 'white noise' initial conditions, $\langle\phi(\mathbf{x}, 0)\phi(\mathbf{x}', 0)\rangle = \delta^d(\mathbf{x} - \mathbf{x}')$, this takes the form

$$a(t_1, t_2) \equiv \langle X(t_1)X(t_2)\rangle = [4t_1t_2/(t_1 + t_2)^2]^{d/4}. \tag{127}$$

More generally, this form is asymptotically correct provided the initial condition correlator is sufficiently short-ranged (it must decrease faster than $|\mathbf{x} - \mathbf{x}'|^{-d}$).

Introducing the new time variable $T = \ln t$, one sees that the autocorrelation function becomes $a(T_1, T_2) = f(T_1 - T_2)$, where $f(T) = [\mathrm{sech}(T/2)]^{d/2}$. Thus the process $X(T)$ is *stationary* (the gaussian nature of the process ensures that all higher-order correlators are also time-translation invariant). This is an important simplification. Note that the anticipated form of the probability of $X(t)$ having no zeros between t_1 and t_2, $p_0(t_1, t_2) \sim (t_1/t_2)^\theta$ for $t_2 \gg t_1$, becomes an exponential decay, $p_0 \sim \exp[-\theta(T_2 - T_1)]$, in the new time variable. This reduces the calculation of an exponent to the calculation of a decay rate[98]. The only approximation we shall make is that the intervals between successive zeros of $X(T)$ are statistically independent. This 'independent interval approximation' (IIA) was introduced in another

context some forty years ago [104]. We shall show that it is an extraordinarily good approximation for the diffusion equation.

4.2.1 The Independent Interval Approximation

As a preliminary step, we introduce the 'clipped' variable $\sigma = \text{sign}(X)$, which changes sign at the zeros of $X(t)$. Clearly, the correlator $A(T) = \langle\sigma(0)\sigma(T)\rangle$ is determined solely by the distribution $P(T)$ of the intervals between zeros. The strategy is to determine $P(T)$ from $A(T)$, and p_0(T) from $P(T)$. To this end we note first that

$$A(T) = \frac{2}{\pi}\sin^{-1}[(a(T)] = \frac{2}{\pi}\sin^{-1}\left([\text{sech}\,(\text{T}/2)]^{\text{d}/2}\right), \tag{128}$$

where the first equality holds for any gaussian process.

Next one expresses $A(T)$ in terms of the interval-size distribution $P(T)$. Clearly

$$A(T) = \sum_{n=0}^{\infty}(-1)^n p_n(T), \tag{129}$$

where $p_n(T)$ is the probability that the interval T contains n zeros of $X(T)$. We define $Q(T)$ to be the probability that an interval of size T to the right or left of a zero contains no further zeros. Then $P(T) = -Q'(T)$. For $n \geq 1$ one obtains immediately

$$p_n(T) = \langle T\rangle^{-1}\int_0^T dT_1\int_{T_1}^T dT_2\ldots\int_{T_{n-1}}^T dT_n\, Q(T_1)P(T_2{-}T_1)\ldots P(T_n{-}T_{n-1})Q(T{-}T_n), \tag{130}$$

where $\langle T\rangle$ is the mean interval size. One has made the IIA by writing the joint distribution of n successive zero-crossing intervals as the product of the distribution of single intervals. Taking Laplace transforms gives $\tilde{p}_n(s) = [\tilde{Q}(s)]^2[\tilde{P}(s)]^{n-1}/\langle T\rangle$. But $P(T) = -Q'(T)$ implies $\tilde{P}(s) = 1 - s\tilde{Q}(s)$, where we have used $Q(0) = 1$. Using this to eliminate $\tilde{Q}(s)$ gives the final result

$$\tilde{p}_n(s) = \frac{1}{\langle T\rangle s^2}\left(1-\tilde{P}(s)\right)^2\left(\tilde{P}(s)\right)^{n-1}, \quad n \geq 1, \tag{131}$$

$$= \frac{1}{\langle T\rangle s^2}\left(\langle T\rangle s - 1 + \tilde{P}(s)\right), \quad n = 0, \tag{132}$$

where the result for $\tilde{p}_0(s)$ follows from the normalization condition $\sum_{n=0}^{\infty} p_n(t) = 1$, which gives $\sum_{n=1}^{\infty}\tilde{p}_n(s) = 1/s$.

Finally the Laplace transform of (129) gives $\tilde{A}(s) = \sum_{n=0}^{\infty}(-1)^n\tilde{p}_n(s)$. Performing the sum employing (131) and (132), and using the result to express $\tilde{P}(s)$ in terms of $\tilde{A}(s)$ gives the desired result

$$\tilde{P}(s) = [2 - F(s)]/F(s), \tag{133}$$

where

$$F(s) = 1 + (\langle T\rangle/2)\, s[1 - s\tilde{A}(s)]. \tag{134}$$

Equations (131-134) are a general consequence of the independent interval approximation. The function $F(s)$, defined by (134), is completely determined by the autocorrelation function $A(T)$, and contains all the information needed to compute the probabilities $p_n(T)$. We have in mind, of course, to apply this approach to the diffusion equation, where $A(T)$ is given by (128). For this case the mean interval size $\langle T\rangle$, required in (134), can be simply evaluated. For $T \to 0$, the probability

to find a zero in the interval T is just $T/\langle T\rangle$, so $A(T) \to 1 - 2T/\langle T\rangle$. This gives $\langle T\rangle = -2/A'(0) = \pi\sqrt{8/d}$, using (128) in the final step.

We note a very important point at this stage. The fact that $A'(0)$ is finite (i.e. $f'(0) = 0$ and $f''(0) \neq 0$) is special to the diffusion equation, which allows us to use the IIA. Physically this means that the density of zeros is a finite number. However, for many Gaussian stationary processes $f'(0) \neq 0$, implying that $A'(0)$ diverges. In this case, the IIA cannot be used. For such processes, the variational and perturbative methods developed in Ref.[98, 103] give reasonably accurate results.

The asymptotics of $p_0(T)$ are controlled by the singularity of $\tilde{p}_0(s)$ with the largest real part, i.e. [from (132)] by the corresponding singularity of $\tilde{P}(s)$. The expectation that $p_0(T) \sim \exp(-\theta T)$ suggests that this singularity is a simple pole, i.e. that $F(s)$ has a simple zero at $s = -\theta$. Using (128) in (134), and inserting $\langle T\rangle = \pi\sqrt{8/d}$, gives

$$F(s) = 1 + \pi\left(\frac{2}{d}\right)^{1/2} s\left[1 - \frac{2s}{\pi}\int_0^\infty dT\, \exp(-sT)\sin^{-1}\left(\mathrm{sech}^{d/2}\left(\frac{T}{2}\right)\right)\right] \qquad (135)$$

Clearly $F(0) = 1$, while $F(s)$ diverges to $-\infty$ for $s \to -d/4$. Between these two points $F(s)$ is monotonic, implying a single zero in the interval $(-d/4, 0)$. Solving (135) numerically for this zero, and identifying the result with $-\theta$, gives the values of θ shown in table 2. For future reference, we note from (133) that the residue R of the corresponding pole of $\tilde{P}(s)$ is $R = 2/F'(-\theta)$. The values of R, which controls the amplitude of the asymptotic decay of $p_n(T)$, are also given in table 2. Recall that the behavior $p_0(T) \sim \exp(-\theta T)$ translates in 'real' time to a decay law $p_0(t) \sim t^{-\theta}$ for the probability that ϕ at a given point has not changed sign. It is also easy to extract the large-d behaviour of θ from Eq. (9): we find, to leading order in d, $\theta \approx 0.145486\sqrt{d}$.

d	θ_{th}	θ_{sim}	R
1	0.1203	0.1207 ± 0.0005	0.1277
2	0.1862	0.1875 ± 0.0010	0.2226
3	0.2358	0.2380 ± 0.0015*	0.2940
4	0.2769	–	0.3527
5	0.3128	–	0.4033

Table 2: Exponents θ from theory (θ_{th}) and simulations (θ_{sim}), and the value of the residue R (see text), for various spatial dimensions d. The '$d = 3$' simulation result (*) refers to a $d = 1$ simulation with correlated initial conditions (see text).

4.2.2 Simulations

The predicted values of θ were tested in $d = 1$ and 2 by numerical simulations. The diffusion equation was discretized in space and time in the form

$$\phi_i(t+1) = \phi_i(t) + a\sum_j[\phi_j(t) - \phi_i(t)], \qquad (136)$$

where j runs over the nearest neighbors of i on a linear ($d = 1$) or square ($d = 2$) lattice. A stability analysis shows that the solution is unstable for $a \geq a_c = 1/(2d)$. Preliminary studies showed that the asymptotic exponent is independent of a for $a < a_c$, but that a value $a = a_c/2$ seems to give the quickest onset of the asymptotic behavior. This value was therefore used in all simulations reported here. Systems of 2^{20} (2^{24}) sites were studied in $d = 1$ ($d = 2$), for times up to 2^{17} (2^{12}). Data for longer times in $d = 2$ suffer from noticeable finite-size effects. The initial values of ϕ_i were chosen independently from a gaussian distribution of zero mean. Using

a rectangular distribution gave the same asymptotic exponent within the errors. Several random number generators were tried: All gave consistent results (within the errors).

The simulation results are presented in table 2 (see [90] for more details of the simulations). The agreement with the theoretical predictions is quite remarkable, showing that the IIA is an extraordinarily good approximation in this context.

The case of correlated initial conditions is also of interest. If the Fourier-space correlations are $\langle \phi_{\mathbf{k}}(0)\phi_{-\mathbf{k}}(0)\rangle \sim k^{\sigma}$ for $k \to 0$ ($\sigma > -d$), the autocorrelation function of $X(t)$ still has the form (127), but with d replaced by $d+\sigma$. Therefore, the dependence of θ on d and σ enters only through the combination $d+\sigma$. Results for $d=3$ (and uncorrelated initial conditions) were obtained by simulating a $d=1$ system with $\sigma = 2$, noting that $\sigma = 2$ corresponds in real space to differentiating uncorrelated initial conditions (or taking finite differences on a lattice). The result was $\theta = 0.2380 \pm 0.0015$, close to the predicted result 0.2358 from the IIA.

4.2.3 n-Flip Probabilities

The asymptotics of the probability $p_n(t_1,t_2)$ for having n zeros between times t_1 and t_2 are also readily calculable within the IIA. From (131) and (132), the singularity in $\tilde{p}_n(s)$ as $s=-\theta$ is an $(n+1)^{\text{th}}$-order pole of strength $R^{n+1}/\langle T\rangle\theta^2$, where R is the strength of the simple pole in $\tilde{P}(s)$. Inverting the Laplace transform, and retaining only the leading large-T behavior, gives (for all n)

$$p_n(T) \to \frac{R}{\langle T\rangle\theta^2}\,\frac{(RT)^n}{n!}\,\exp(-\theta T). \tag{137}$$

With $T=\ln(t_2/t_1)$, one obtains

$$p_n(t_1,t_2) \to (R^{n+1}/\langle T\rangle\theta^2)\,[\ln(t_2/t_1)]^n\,(t_1/t_2)^{\theta}. \tag{138}$$

When the time t_1 corresponds to the initial condition, one has to set t_1 equal to a constant of order unity, as was implicit in the earlier treatment of $p_0(t)$. Setting $t_2 = t$ one then gets $p_n(t) \sim (\ln t)^n\, t^{-\theta}$. Simulations are consistent with this form, at least for n not too large [108].

4.3 Discussion

We turn to a brief discussion of the experimental relevance of our results. The ubiquity of the diffusion equation in physics implies that applications will be many and varied. Our first example is the coarsening dynamics of a nonconserved scalar order parameter, which was our original motivation. The twisted nematic liquid crystal film provides a convenient experimental realization. The exponent theta for this $d=2$ system has recently been measured, with the result $\theta = 0.19 \pm 0.03$ [105], in good agreement with the result $\theta \simeq 0.19$ from the OJK theory (table 2). Actually, the agreement is better than might be expected: a measurement of the autocorrelation exponent $\bar{\lambda}$ on the same system gave $\bar{\lambda} \simeq 1.25$ [17], quite different from the prediction $\bar{\lambda} = d/2 = 1$ of the OJK theory.

As a second example consider the reaction-diffusion process $A+B \to C$, where C is inert and immobile. The corresponding rate equations for the concentrations are $dn_A/dt = \nabla^2 n_A - R$, $dn_B/dt = \nabla^2 n_B - R$, and $dn_C/dt = R$, where R is the reaction rate per unit volume ($R \propto n_A n_B$ for $d > 2$ [106]). The concentration difference, $\Delta n \equiv n_A - n_B$, obeys the diffusion equation exactly. If the A and B species are randomly mixed at $t=0$ the system evolves, for $d < d_c = 4$, to a coarsening state in which the two species segregate into domains [107], separated by domain walls whose locations are defined by $\Delta n = 0$. Subsequent production of the inert species C is slaved to the motion of the domain walls, which are zeros of the diffusion field Δn. The fraction of space not infected by the C species will therefore decay asymptotically as $t^{-\theta}$.

We conclude with some other examples of non-trivial exponents θ that have recently been discussed. The first is associated with the dynamics of the *global* order parameter $M(t)$ (e.g. the total magnetization of an Ising ferromagnet) at a critical point T_c, following a quench to T_c from the high-temperature phase. The quench prepares the system in a state with random initial conditions. In the subsequent evolution (now stochastic, rather than deterministic), the probability that $M(t)$ has not changed sign since $t = 0$ decays as $t^{-\theta_c}$, where θ_c is a *new critical exponent* [102, 103]. For reasons similar to those given for the diffusion problem, we expect θ_c to be an independent exponent, i.e. not related by any scaling law to the usual static and dynamic exponents. As a second example, one can consider $M(t)$ for a quench to $T = 0$ from high temperature. In this case, $p_0(t) \sim t^{-\theta_0}$, where θ_0 differs from the corresponding exponent for single spins. For the $d = 1$ Glauber model, for example, the probability that $M(t)$ has not changed sign decays with an exponent $\theta_0 = 1/4$ [102], which differs from the exponent 3/8 obtained for the zero-flip probability of a given spin [97].

As a final example, consider the generalised one-dimensional random-walk equation $d^n x/dt^n = \xi(t)$, where ξ is gaussian white noise. The cases $n = 1, 2, \ldots$ correspond to a random velocity (the usual random walk), random acceleration, etc. The first two θ_n are $\theta_1 = 1/2$ and $\theta_2 = 1/4$ [109], but larger n have not been considered before to our knowledge. Application of the independent interval approximation [108] gives equations of the same structure as for the diffusion process, but with $\mathrm{sech}^d(T/2)$ in (128) and (135) replaced by $(2 - 1/n)\exp(-T/2)\,{}_2F_1[1, 1 - n; 1 + n; \exp(-T)]$, where ${}_2F_1$ is the hypergeometric function. This approach gives $\theta_2 = 0.2647$ (instead of 1/4) while, for larger n, θ_n approaches a limiting value $\theta_\infty = 0.1862\ldots$, i.e. the same exponent as the $d = 2$ diffusion equation! In fact, the equality of the exponents for the $n = \infty$ process and $d = 2$ diffusion can be proved exactly [108], implying a limiting exponent 0.1875 ± 0.0010 (from table 2) for the former.

To summarize, we have discussed persistence in the context of the diffusion equation or, equivalently, the OJK theory of ordering kinetics. The key factor underlying the nontriviality of θ is that the dynamics of $\phi(\mathbf{x})$ for a particular point $\mathbf{x}$ is *non-Markovian.* (The autocorrelation function $A(T)$ of any gaussian *Markov* process, expressed in the stationary variable T, is a simple exponential: $A(T) = \exp(-\mu T)$. For this case one can show that the persistence probability is $p(T) = (2/\pi)\sin^{-1}[A(T)]$ exactly, i.e. $\theta = \mu$ for a gaussian Markov process. Any non-exponential form for $A(T)$ implies a non-Markov process.) We have introduced the Independent Interval Approximation as a useful tool for estimating θ in cases where the density of zeros is finite. When the density is infinite, other techniques are necessary. A recent preprint [110] introduces a variety of such techniques in the context of the dynamics of fluctuating interfaces.

As a final remark we note that, quite generally, the set of persistent sites is a *fractal set*, with fractal dimension $D = d - \theta/z$, up to the coarsening scale $L(t) \sim t^{1/z}$. Consider two points a distance r apart, with the first point chosen from the persistent set. Let $p(r, t)$ be the probability that the second point also belongs to the persistent set. For $r \gg L(t)$, the two points are uncorrelated, giving $p(t) \sim t^{-\theta}$. For general r and t, scaling implies $p(r, t) = t^{-\theta} g(r/t^{1/z})$. But for $r \ll t^{1/z}$, p should become independent of t, so $g(x) \sim x^{-\theta/z}$ for $x \to 0$. It follows that $p(r, t) \sim r^{-\theta/z}$ for $r \ll L(t)$. The number of persistent sites within a radius R of a given persistent site is therefore of order $R^{d-\theta/z}$, for $R \ll L(t)$, giving the fractal dimension as $D = d - \theta/z$. This result has been confirmed for the diffusion equation ($z = 2$) in one [111] and two [112] dimensions.

References

[1] A. J. Bray, Adv. Phys. **43**, 357 (1994).

[2] A. J. Bray, Comments Cond. Mat. Phys. **14**, 21 (1988).

[3] J. S. Langer, in *Solids Far From Equilibrium*, ed. C. Godrèche (Cambridge, Cambridge, 1992).

[4] P. C. Hohenberg and B. I. Halperin, Rev. Mod. Phys. **49**, 435 (1977).

[5] A. J. Bray, Phys. Rev. Lett. **62**, 2841 (1989).

[6] A. J. Bray, Phys. Rev. B **41**, 6724 (1990).

[7] K. Binder and D. Stauffer, Phys. Rev. Lett. **33**, 1006 (1974).

[8] J. Marro, J. L. Lebowitz and M. H. Kalos, Phys. Rev. Lett. **43**, 282 (1979).

[9] H. Furukawa, Prog. Theor. Phys. **59**, 1072 (1978).

[10] H. Furukawa, Phys. Rev. Lett. **43**, 136 (1979).

[11] A. J. Bray, J. Phys. A **22**, L67 (1990); J. G. Amar and F. Family, Phys. Rev. A **41**, 3258 (1990). See also B. Derrida, C. Godrèche and I. Yekutieli, Phys. Rev. A **44**, 6241 (1991).

[12] A. Coniglio and M. Zannetti, Europhys. Lett. **10**, 575 (1989).

[13] H. Furukawa, J. Phys. Soc. Jpn. **58**, 216 (1989).

[14] H. Furukawa, Phys. Rev. B **40**, 2341 (1989).

[15] D. S. Fisher and D. A. Huse, Phys. Rev. B **38**, 373 (1988). Note that our exponent $\bar{\lambda}$ is called λ in this paper.

[16] T. J. Newman and A. J. Bray, J. Phys. A **23**, 4491 (1990).

[17] N. Mason, A. N. Pargellis, and B. Yurke, Phys. Rev. Lett. **70**, 190 (1993); for earlier work on twisted nematics see H. Orihara and Y. Ishibashi, J. Phys. Soc. Jpn. **55**, 2151 (1986); T. Nagaya, H. Orihara and Y. Ishibashi, *ibid.* **56**, 1898 (1987); **56**, 3086 (1987); **59**, 377 (1990).

[18] G. Porod, Kolloid Z. **124**, 83 (1951); **125**, 51 (1952).

[19] P. Debye, H. R. Anderson and H. Brumberger, J. Appl. Phys. **28**, 679 (1957); G. Porod, in *Small-Angle X-Ray Scattering*, edited by O. Glatter and O. Kratky (Academic, New York, 1982).

[20] S. M. Allen and J. W. Cahn, Acta. Metall. **27**, 1085 (1979).

[21] D. A. Huse, Phys. Rev. B **34**, 7845 (1986).

[22] J. Amar, F. Sullivan and R. Mountain, Phys. Rev. B **37**, 196 (1988); T. M. Rogers, K. R. Elder and R. C. Desai, Phys. Rev. B **37**, 9638 (1988); R. Toral, A. Chakrabarti and J. D. Gunton, Phys. Rev. B **39**, 4386 (1989); C. Roland and M. Grant, Phys. Rev. B **39**, 11971 (1989).

[23] A. J. Bray and A. D. Rutenberg, Phys. Rev. E **49**, R27 (1994).

[24] A. D. Rutenberg and A. J. Bray, Phys. Rev. E **51**, 5499 (1995).

[25] For a general discussion of topological defects, see e.g. M. Kléman, *Points, Lines and Walls, in Liquid Crystals, Magnetic Systems, and Various Ordered Media* (Wiley, New York, 1983).

[26] See, for example, S. Ostlund, Phys. Rev. B **24**, 485 (1981).

[27] A. N. Pargellis, P. Finn, J. W. Goodby, P. Pannizza, B. Yurke and P. E. Cladis, Phys. Rev. A **46**, 7765 (1992).

[28] B. Yurke, A. N. Pargellis, T. Kovacs and D. A. Huse, Phys. Rev. E **47**, 1525 (1993).

[29] I am grateful to N. Turok for a useful discussion of this approach.

[30] C. D. Musny and N. A. Clark, Phys. Rev. Lett. **68**, 804 (1992); H. Pleiner, Phys. Rev. A **37**, 3986 (1988); P. E. Cladis, W. van Sarloos, P. L. Finn and A. R. Kortan, Phys. Rev. Lett. **58**, 222 (1987); G. Ryskin and M. Kremenetsky, Phys. Rev. Lett. **67**, 1574 (1991); A. Pargellis, N. Turok and B. Yurke, Phys. Rev. Lett. **67**, 1570 (1991).

[31] L. M. Pismen and B. Y. Rubinstein, Phys. Rev. Lett. **69**, 96 (1992).

[32] A. J. Bray, Phys. Rev. E **47**, 228 (1993).

[33] A. J. Bray and K. Humayun, Phys. Rev. E **47**, R9 (1993).

[34] A. J. Bray and S. Puri, Phys. Rev. Lett. **67**, 2670 (1991).

[35] H. Toyoki, Phys. Rev. B **45**, 1965 (1992).

[36] Fong Liu and G. F. Mazenko, Phys. Rev. B **45**, 6989 (1992).

[37] A. J. Bray and K. Humayun, J. Phys. A **25**, 2191 (1992).

[38] G. F. Mazenko and M. Zannetti, Phys. Rev. Lett. **53**, 2106 (1984); Phys. Rev. B **32**, 4565 (1985); M. Zannetti and G. F. Mazenko, Phys. Rev. B **35**, 5043 (1987); F. de Pasquale in *Nonequilibrium Cooperative Phenomena in Physics and Related Topics*, p. 529, edited by M. G. Velarde (New York, Plenum, 1984); F. de Pasquale, D. Feinberg and P. Tartaglia, Phys. Rev. B **36**, 2220 (1987).

[39] A. Coniglio, P. Ruggiero and M. Zannetti, Phys. Rev. E **50**, 1046 (1994). This paper contains a rather complete discussion of growth kinetics in the large-n limit, for both nonconserved and conserved dynamics.

[40] T. J. Newman, A. J. Bray, and M. A. Moore, Phys. Rev. B **42** 4514, (1990).

[41] J. G. Kissner and A. J. Bray, J. Phys. A **26**, 1571 (1993). Note that this paper corrects an error in reference [16].

[42] A similar exponent has been introduced in the context of nonequilibrium *critical* dynamics by H. K. Janssen, B. Schaub and B. Schmittman, Z. Phys. **73**, 539 (1989).

[43] Note that the exponent λ defined here (and in earlier papers by the author) differs from that defined in reference [15] and in the papers of Mazenko: the exponent λ defined in these papers is our $\bar{\lambda}$.

[44] A. J. Bray, K. Humayun and T. J. Newman, Phys. Rev. B **43**, 3699 (1991).

[45] T. Ohta, D. Jasnow and K. Kawasaki, Phys. Rev. Lett. **49**, 1223 (1982).

[46] C. Yeung and D. Jasnow, Phys. Rev. B **42**, 10523 (1990).

[47] Y. Oono and S. Puri, Mod. Phys. Lett. B **2**, 861 (1988).

[48] K. Kawasaki, M. C. Yalabik and J. D. Gunton, Phys. Rev. A **17**, 455 (1978).

[49] G. F. Mazenko, Phys. Rev. Lett. **63**, 1605 (1989).

[50] G. F. Mazenko, Phys. Rev. B **42**, 4487 (1990).

[51] G. F. Mazenko, Phys. Rev. B **43**, 5747 (1991).

[52] A. J. Bray and K. Humayun, Phys. Rev. E **48**, 1609 (1993).

[53] M. Suzuki, Prog. Theor. Phys. **56**, 77 (1976); **56**, 477 (1976).

[54] S. Puri and C. Roland, Phys. Lett. A **151**, 500 (1990).

[55] K. Humayun and A. J. Bray, Phys. Rev. B **46**, 10594 (1992).

[56] F. Liu and G. F. Mazenko, Phys. Rev. B **44**, 9185 (1991).

[57] A. J. Bray and K. Humayun, Phys. Rev. Lett. **68**, 1559 (1992).

[58] K. Humayun and A. J. Bray, J. Phys. A **24**, 1915 (1991).

[59] A. J. Bray and K. Humayun, J. Phys. A **23**, 5897 (1990).

[60] F. Liu and G. F. Mazenko, Phys. Rev. B **45**, 4656 (1992).

[61] C. Yeung, Y. Oono and A. Shinozaki, Phys. Rev. E **49**, 2693 (1994).

[62] G. F. Mazenko, Phys. Rev. E **49**, 3717 (1994).

[63] A. J. Bray and J. G. Kissner, J. Phys. A **25**, 31 (1992).

[64] D. A. Huse and C. L. Henley, Phys. Rev. Lett. **54**, 2708 (1985).

[65] J. Villain, Phys. Rev. Lett. **52**, 1543 (1984).

[66] R. Bruinsma and G. Aeppli, Phys. Rev. Lett. **52**, 1543 (1984).

[67] T. Nattermann, Phys. Status Solidi b **132**, 125 (1985).

[68] D. A. Huse, C. L. Henley and D. S. Fisher, Phys. Rev. Lett. **5**, 2924 (1985).

[69] G. S. Grest and D. J. Srolovitz, Phys. Rev. B **32**, 3014 (1985); D. Chowdhury, M. Grant and J. D. Gunton, Phys. Rev. B **35**, 6792 (1985); D. Chowdhury and S. Kumar, J. Stat. Phys. **49**, 855 (1987); J. H. Oh and D. I. Choi, Phys. Rev. B **33**, 3448 (1986); D. Chowdhury, J. Physique **51**, 2681 (1990).

[70] A. J. Bray and K. Humayun, J. Phys. A **24**, L1185 (1991).

[71] S. Puri, D. Chowdhury and N. Parekh, J. Phys. A **24**, L1087 (1991).

[72] A. G. Schins, A. F. M. Arts and H. W. de Wijn, Phys. Rev. Lett. **70**, 2340 (1993).

[73] M. Rao and A. Chakrabarti, Phys. Rev. Lett. **71**, 3501 (1993).

[74] A. J. Bray, Phys. Rev. Lett. **62**, 2841 (1989); Phys. Rev. B **41**, 6724 (1990).

[75] S. Puri and N. Parekh, J. Phys. A **15**, 4127 (1992).

[76] T. Iwai and H. Hayakawa, J. Phys. Soc. Jpn. **62**, 1583 (1993); H. Hayakawa and T. Iwai, in *Pattern Formation in Complex Dissipative Systems*, edited by S. Kai (World Scientific, 1992).

[77] J. R. Banavar and M. Cieplak, Phys. Rev. Lett. **48**, 832 (1982); Phys. Rev. B **26**, 2662 (1982); **28**, 3813 (1984); M. Cieplak and J. R. Banavar, *ibid.* **27**, 293 (1983); **29**, 469 (1984).

[78] A. J. Bray and M. A. Moore, J. Phys. C **17**, L463 (1984).

[79] A. J. Bray and M. A. Moore, J. Phys. C **17**, L613 (1984).

[80] A. J. Bray and M. A. Moore, in *Heidelberg Colloquium on Glassy Dynamics and Optimization*, eds. L. van Hemmen and I Morgenstern, Lecture Notes in Physics vol. 275 (Springer-Verlag, Berlin, 1987).

[81] W. L. McMillan, J. Phys. C **17**, 3179 (1984); Phys. Rev. B **29**, 4026 (1984); Phys. Rev. B **29**, 4026 (1984).

[82] R. G. Caflisch, J. R. Banavar and M. Cieplak, J. Phys. C **18**, L991 (1985).

[83] D. S. Fisher and D. A. Huse, Phys. Rev. Lett. **58**, 57 (1996).

[84] J. R. Banavar and A. J. Bray, Phys. Rev. B **35**, 8888 (1987).

[85] J. R. L. de Almeida and D. J. Thouless, J. Phys. A **11**, 983 (1978).

[86] Y. Imry and S.-K. Ma, Phys. Rev. Lett. **35**, 1399 (1975).

[87] A. J. Bray and M. A. Moore, Phys. Rev. Lett. **58**, 57 (1987).

[88] D. A. Huse, Phys. Rev. B **43**, 8673 (1991).

[89] B. Derrida, Phys. Rev. E **55**, 3705 (1997).

[90] S. N. Majumdar, C. Sire, A. J. Bray and S. J. Cornell, Phys. Rev. Lett. **77**, 2867 (1996).

[91] B. Derrida, V. Hakim, and R. Zeitak, Phys. Rev. Lett. **77**, 2871 (1996).

[92] B. Derrida, A. J. Bray, and C. Godrèche, J. Phys. A **27**, L357 (1994).

[93] A. J. Bray, B. Derrida, and C. Godrèche, Europhys. Lett. **27**, 175 (1994).

[94] D. Stauffer, J. Phys. A **27**, 5029 (1994).

[95] B. Derrida, P. M. C. de Oliveira, and D. Stauffer, Physics A **224**, 604 (1996).

[96] E. Ben-Naim, L. Frachebourg, and P. L. Krapivsky, Phys. Rev. E **53**, 3078 (1996).

[97] B. Derrida, V. Hakim, and V. Pasquier, Phys. Rev. Lett. **75**, 751 (1995).

[98] S. N. Majumdar and C. Sire, Phys. Rev. Lett. **77**, 1420 (1996).

[99] S. J. Cornell and A. J. Bray, Phys. Rev. E **54**, 1153 (1996).

[100] J. Cardy, J. Phys. A, **28**, L19 (1995).

[101] E. Ben-Naim, P. L. Krapivsky, and S. Redner, Phys. Rev. E **50**, 2474 (1994).

[102] S. N. Majumdar, A. J. Bray, S. J. Cornell and C. Sire, Phys. Rev. Lett. **77**, 3704 (1996).

[103] K. Oerding, S. J. Cornell and A. J. Bray, Phys. Rev. E **56**, 25R (1997).

[104] J. A. McFadden, IRE Transaction on Information Theory, IT-4, p.14 (1957).

[105] B. Yurke, A. N. Pargellis, S. N. Majumdar and C. Sire, Phys. Rev. E **56**, R40 (1997).

[106] S. J. Cornell and M. Droz, Phys. Rev. Lett. **70**, 3824 (1993); B. P. Lee and J. Cardy, J. Stat. Phys. **80**, 971 (1995).

[107] D. Toussaint and F. Wilczek, J. Chem. Phys. **78**, 2642 (1978).

[108] A. J. Bray, S. J. Cornell, S. N. Majumdar, and C. Sire, unpublished.

[109] T. W. Burkhardt, J. Phys. A **26**, L1157 (1993); Y. G. Sinai, Theor. Math. Phys. **90**, 219 (1992); A. C. Maggs, D. A. Huse, and S. Leibler, Europhys. Lett. 615 (1989).

[110] J. Krug, H. Kallabis, S. N. Majumdar, S. J. Cornell, A. J. Bray and C. Sire, to appear in Phys. Rev. E.

[111] D. H. Zanette, Phys. Rev. E **55**, 2462 (1997).

[112] S. J. Cornell, unpublished.

FIGURES

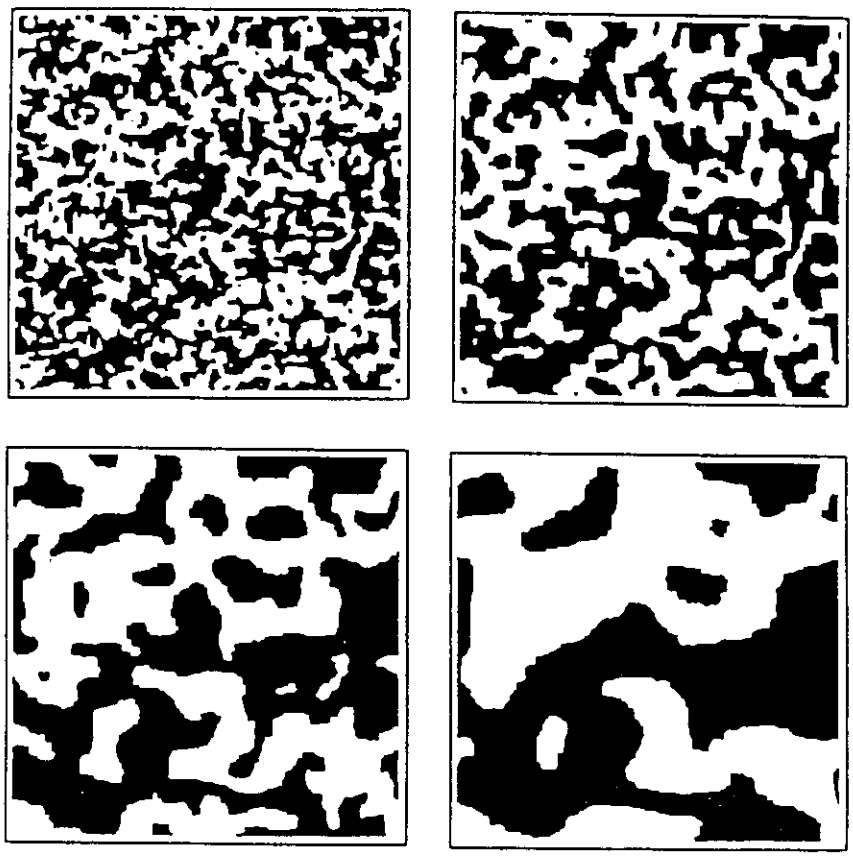

Figure 1 Monte Carlo simulation of domain growth in the $d = 2$ Ising model at $T = 0$ (taken from Kissner [8]). The system size is 256×256, and the snapshots correspond to 5, 15, 60 and 200 Monte Carlo steps per spin after a quench from $T = \infty$.

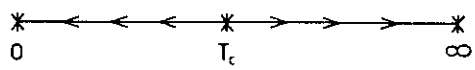

Figure 2 Schematic RG flow diagram, with fixed points at $T = 0$, T_C and ∞. All $T > T_C$ are equivalent to $T = \infty$ and all $T < T_C$ to $T = 0$, as far as large length-scale properties are concerned.

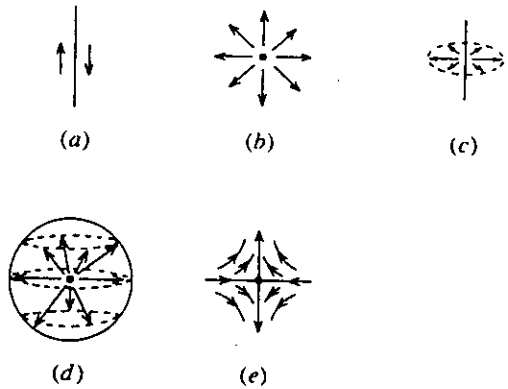

Figure 3 Types of topological defect in the O(n) model: (a) domain wall ($n = 1$); (b) vortex ($n = 2 = d$); (c) string ($n = 2$; $d = 3$); (d) monopole or 'hedgehog' ($n = 3 = d$); (e) antivortex.

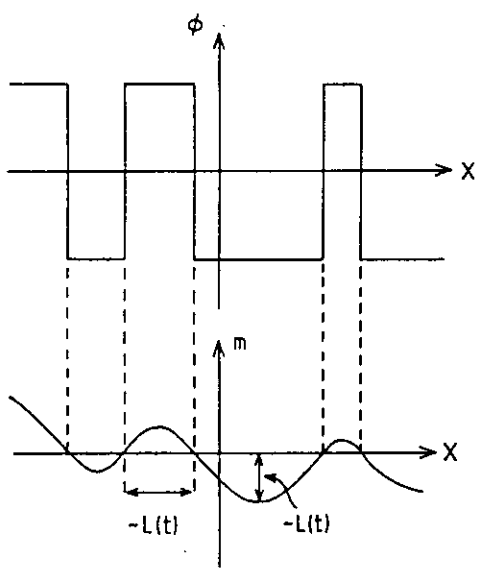

Figure 4 Spatial variation (schematic) of the order parameter ϕ and the auxiliary field m.

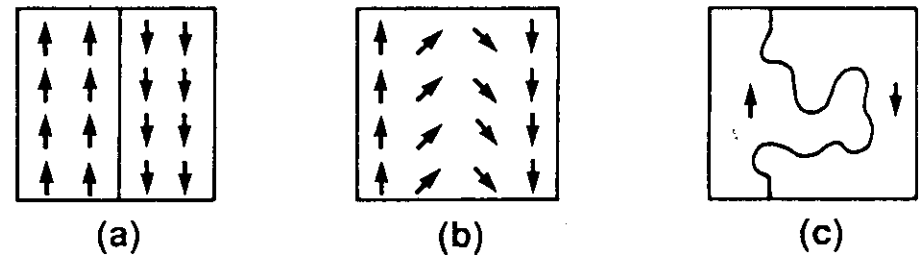

FIGURE 5 Examples of the spin "textures" formed in two-dimensional samples at zero temperature when antiperiodic boundary conditions are imposed in the horizontal direction. Periodic boundary conditions are assumed in the vertical direction. (a) Ising ferromagnet. (b) Heisenberg ferromagnet. (c) Ising spin glass. In this case the arrows indicate spin directions relative to the ground state for fully periodic boundary conditions. For the Ising systems (a) and (c), the antiperiodic boundary conditions lead to a "domain wall" separating spins that change direction under a change of boundary conditions from those that don't. For the spin glass, the domain wall energy is equally likely to be positive or negative. (The latter corresponds to a *lower* energy for antiperiodic boundary conditions.)

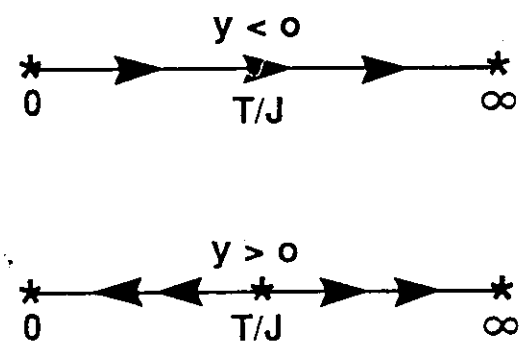

FIGURE 6 Schematic Renormalization Group flows. For $y > 0$ the zero-temperature fixed point is *stable* with respect to temperature, implying an ordered phase at low temperature. For $y < 0$ it is *unstable*, implying a disordered phase.